

PRIMARY RESEARCH ARTICLE

Climate-change-driven shifts in the population dynamics of the invasive tiger mosquito (*Aedes albopictus*) in the Alps

Margo Blaha¹ | Michael Matiu² | Bruno Majone² | Dino Zardi^{1,2} | Eleonora Flacio^{3,4} |
Nikoleta Anicic^{3,4} | Swiss Mosquito Network | Annapaola Rizzoli⁵ | Alberta Stenico⁶ |
Filippo Cassina⁶ | Roberto Rosà*¹ | Daniele Da Re*⁵

¹Center Agriculture Food Environment, University of Trento, S. Michele all'Adige (TN), Italy

²Department of Civil, Environmental and Mechanical Engineering (DICAM), University of Trento, Trento (TN), Italy

³Institute of Microbiology, University of Applied Sciences and Arts of Southern Switzerland (SUPSI), Mendrisio, Switzerland

⁴Swiss Mosquito Network, Switzerland

⁵Research and Innovation Centre, Fondazione Edmund Mach, S. Michele all'Adige (TN), Italy

⁶Biological Laboratory, Provincial Agency for the Environment and Climate Protection, Laives (BZ), Italy

Correspondence

Corresponding author: Margo Blaha

Email: margo.blaha@unitn.it

Abstract

The recent global expansion of the Asian tiger mosquito (*Aedes albopictus*) across tropical and temperate regions provides a clear example of the mobility and adaptability of invasive species. Among multiple drivers influencing the spread of this species, climate change is emerging as a major driver, creating conditions that favour its persistence and expansion into higher latitudes and elevations. Hence, as global warming continues to make the climate of mountain areas milder, understanding *Ae. albopictus*' range and seasonality expansion in the Alpine area is fundamental, as it could introduce and propagate mosquito-borne diseases in previously free areas. Our objective is to evaluate the likely impact of climate change on the distribution and seasonality of *Ae. albopictus* for the periods 2036-2055 and 2066-2085 in the Alps. We use entomological data collected for public health surveillance, along with temperature and precipitation datasets from surface observations and regional climate model simulations, to train a machine-learning mosquito population model and predict its spatial distribution under both current and future climate conditions. Our results demonstrate how increasing temperatures and altered precipitation regimes increase the abundance and seasonal expansion of *Ae. albopictus*. In particular, rising temperatures are projected to push the species' range to higher altitudes and to lengthen the duration of climatically suitable conditions. Projected warming increased mean season length by 1.8–3.6 weeks, depending on location, and expanded suitable elevation by several hundred metres across future climates, demonstrating consistent climate-driven increases in both seasonal activity and spatial reach of *Ae. albopictus* in the Alps.

KEYWORDS

climate warming, global change, invasive species, machine learning, mosquito, range shift, species distribution modelling

1 | INTRODUCTION

Mountain regions are among the most sensitive environments to climate change, and the Alps in Europe are no exception. Although they cover only 1.8% of Europe ($\approx 190,000$ km²), the Alps host exceptional ecological and socio-economic diversity and are undergoing some of the continent's most rapid climatic transformations, being the Mediterranean region considered a hot spot for climate change (Kotlarski et al. 2023, Lazoglou et al. 2024). Anthropogenic greenhouse gas emissions have led to an average global near-surface temperature increase of

+1.4°C compared to pre-industrial levels (1850–1900), but Europe is warming at twice the global average rate (IPCC 2021, C3S 2024). In the Alps, mean temperatures have already risen by approximately 2°C above pre-industrial levels, accompanied by subtle shifts in precipitation seasonality, generally towards wetter winters and drier summers in some areas (Dumont et al. 2025, Pepin et al. 2025). Such climatic changes are altering ecological balances and opening opportunities for ectothermic species previously limited by colder temperatures (Paaïmans et al. 2013), including invasive alien species, such as competent disease vectors like *Aedes albopictus* (Skuse, 1894), the Asian tiger mosquito. On a global level, climate projections indicate an additional increase of 1.4 to 4.4°C by 2100, depending on the trajectories of greenhouse gas

* Daniele Da Re and Roberto Rosà should be considered joint senior authors.

emissions (IPCC 2022). European mountain regions are expected to warm even faster than the global mean, with continued intensification of seasonal hydrological contrasts, which means winters getting slightly wetter and summers getting significantly drier (Coppola et al. 2021).

Species respond to climate change in diverse ways, largely determined by their physiological tolerance limits to temperature and precipitation (Cahill et al. 2014, Pacifici et al. 2015). Insects, as ectotherms, are particularly sensitive to climatic variability, and frequently display rapid ecological and phenological adjustments to environmental changes (Paaijmans et al. 2013).

Ae. albopictus has emerged as a major global health concern, due to its potential role in transmitting more than 21 arboviruses, and as a proven vector of at least five arboviruses (Bohers et al. 2024). Native to Southeast Asia, it has demonstrated remarkable plasticity, successfully expanding across all continents except Antarctica. Introduced to Europe in 1979 (Adhami and Reiter 1998), it is now widespread in southern and central Europe, including the Alpine foothills (Roiz et al. 2011, Flacio et al. 2016, Battistin et al. 2024).

This expansion has been facilitated by several biological and environmental factors: *Ae. albopictus* possesses cold-tolerant diapausing eggs, allowing it to overwinter in temperate climates (Hawley 1988, Hanson and Craig Jr 1994, Thomas et al. 2012, Lacour et al. 2014, Tippelt et al. 2019 2020), is highly adaptable to urban and peri-urban habitats, with a preference for container breeding that abounds in human-modified environments (Wilke et al. 2021, Ferraguti et al. 2022), and it has a life cycle tightly linked to climatic signals (Hawley 1988). Consequently, warmer winters and shifting precipitation patterns are making many mountain and pre-mountain environments increasingly suitable for colonisation (Roiz et al. 2011, Neteler et al. 2013, Giunti et al. 2023). Its upward expansion into mid-elevation Alpine zones, now documented up to 600 m above sea level, is closely linked to ongoing climate change (Battistin et al. 2024, Medlock et al. 2015).

Despite the growing presence of *Ae. albopictus* in mountainous Europe, little is known about how future climate trajectories will reshape its elevational limits, seasonal dynamics, and regional abundance in the Alps. While both correlative and mechanistic approaches have been used to explore the potential effects of climate change on mosquito distributions (Proestos et al. 2015, Metelmann et al. 2019), no study has yet provided a comprehensive, spatially and temporally explicit assessment of *Ae. albopictus*' population dynamics across the entire Alpine arc.

In the present paper, we address this gap using a machine-learning framework that is trained and tested on weekly ovitrap observations coupled with historical climate data, and then applied to future climate forcings derived from EURO-CORDEX scenarios to project potential changes in mosquito egg abundance and distribution.

Specifically, our objectives are to:

- Evaluate temporal shifts in seasonal abundance under three distinct climate forcings for mid-century (2036–2055) and late-century (2066–2085) periods.
- Explore the relationship between elevation and projected changes in mosquito egg abundance to assess altitudinal trends in future colonisation risk.

Our results aim to explore how *Ae. albopictus* populations may respond to climate-driven environmental change in mountain landscapes, particularly in areas historically considered unsuitable for invasive mosquito species, providing the first integrative assessment of how climate change is likely to reshape the spatial, temporal, and elevational dynamics of *Ae. albopictus* across the Alps.

2 | METHODS

Our study focuses on the Alps in Europe and surrounding lowland areas, covering parts of Italy, France, Switzerland, Austria, and Slovenia. Geographically, the region is bounded between 43°N and 49°N latitude and 5°E to 18°E longitude. The region is characterised by steep altitudinal gradients—from lowland plains to peaks exceeding 4,000 m—that generate pronounced climatic transitions over short spatial distances. These gradients, coupled with accelerating regional warming (Hock et al. 2019, Boé et al. 2020, Gobiet et al. 2014), make the Alps an ideal setting for examining how climate change influences the spatial and temporal dynamics of *Ae. albopictus*.

2.1 | Data collection

The database for the analysis presented in this paper comes from oviposition trap (ovitrap) sampling. Ovitrap are a standard tool for monitoring *Ae. albopictus* populations. They consist of dark water-filled containers equipped with a rough substrate (usually a wooden or plastic paddle) on which females oviposit, thereby providing a sensitive and standardised index of local reproductive activity. Paddles are retrieved after 1–2 weeks, and eggs are counted under a stereomicroscope, providing a sensitive, cost-effective indicator of local mosquito presence and seasonal dynamics (Focks et al. 2004, Schaffner et al. 2014).

Using this technique, regional surveillance programmes collected ovitrap data across the study area. We compiled these datasets into a harmonised database by standardising sampling frequency, metadata structure, and handling of missing observations. The core dataset comprised ovitrap observations collected from Da Re et al. (2024). To maximise spatial coverage across the Alps, we supplemented these data with additional long-term monitoring efforts:

- Map current spatial patterns of *Ae. albopictus* colonisation and establishment in Alpine and pre-Alpine areas.

- 1 Italy, Autonomous Province of Bolzano: ovitrap data from 2013 to 2024 provided by the Biological Laboratory of the Provincial Agency for the Environment and Climate Protection.
- 2 Switzerland: ovitrap data collected from 2019 to 2024 within the Swiss Mosquito Network, provided by the Institute of Microbiology, University of Applied Sciences and Arts of Southern Switzerland (SUPSI).

Ovitrap sampling is generally continuous, but traps are inspected for the presence and number of eggs at weekly or biweekly intervals, depending on the regional monitoring protocol. To ensure comparability between programs and to match the VectAbundance standards (Da Re et al. 2024), all datasets were standardised to weekly temporal resolution using the `spreader` function in `dynamAedes v2.2.9` (Da Re et al. 2022). This procedure harmonised sampling intervals, recoded winter absences as zeros, and ensured consistent handling of missing or implausible values. Missing sampling weeks were retained as NA values to avoid biasing temporal patterns, but zeros were inserted between November and February to represent winter diapause-related absences (implemented in `spreader`). Erroneous placeholder values (e.g. 999, 9999) were flagged during quality control and recoded as NA.

Ultimately, the final harmonised dataset comprised 49,932 weekly ovitrap records spanning 2010–2024 across the Alps. A detailed breakdown of monitoring sites, spatial coverage, and the number of ovitrap records by region and year is provided in Table A1.

2.1.1 | Environmental data

As environmental predictors for the ML model, we used E-OBS v31.0, a gridded dataset of daily meteorological fields at 0.1° (≈8–11 km) resolution derived from interpolated station observations (Cornes et al. 2018). We extracted climate variables for 20 years (2005–2024), covering beyond the full temporal extent of the ovitrap observations.

From E-OBS, we extracted daily mean air temperature and precipitation, which are variables of established ecological relevance for *Ae. albopictus* development and survival (for further ecological details, see Supplementary Materials 1 in Da Re et al. 2025). Weekly median values were calculated for temperature, and cumulative totals for precipitation. To reflect the known lower thermal constraint for *Ae. albopictus* activity, weekly median temperatures below 15 °C were set to zero prior to modelling. This temperature threshold aligns with experimental and field evidence indicating that *Ae. albopictus* development, activity, and oviposition are strongly reduced below approximately 15 °C (Marini et al. 2020, Reinhold et al. 2018).

Moreover, photoperiod (Toma et al. 2003) was derived at weekly resolution as a deterministic function of latitude and calendar date. For each unique grid-cell centroid, daily day length was calculated using astronomical equations implemented in the `geosphere::daylength` function in R (R Core Team 2025), based solely on latitude and day of year. Daily photoperiod values were then aggregated to the weekly

scale by computing the median day length for each grid cell and epidemiological week. These weekly median photoperiod values were subsequently mapped to the E-OBS grid and temporally aligned with the corresponding climatic covariates.

To capture the delayed and cumulative effects of environmental conditions on ovitrap activity, we represented each covariate using lagged rolling means. Specifically, temperature and photoperiod were represented as weekly medians across week *i* and the 10 preceding weeks (*i*–1 to *i*–10), while precipitation was expressed as cumulative totals across the same window.

2.1.2 | Data alignment and integration

Each ovitrap observation was spatially matched to the corresponding E-OBS grid cell based on its geographic coordinates and temporally aligned to the week of sampling. Because ovitrap monitoring differs in sampling intensity, timing, and spatial density within the E-OBS grid, weekly egg counts were aggregated at the grid-cell level by computing the median of all ovitrap observations falling within the same cell and week. These aggregated mosquito data were then linked to weekly climate variables, ensuring full spatial and temporal consistency between the biological and environmental datasets.

In addition to the grid-based alignment, all observations were assigned to NUTS-2 regions. The NUTS (Nomenclature of Territorial Units for Statistics) classification is the standard spatial framework used by the European Union for regional statistics and policy implementation, with NUTS-2 representing the basic level for regional socio-economic analyses and policy. Labelling observations at the NUTS-2 level allows model outputs and projections to be interpreted within administratively relevant regions, facilitating comparison with public health surveillance, regional planning, and policy-oriented risk assessments.

Ultimately, the integrated dataset comprised 140 unique grid cells across 11 NUTS-2 regions across the Alps (Figure 1).

2.2 | Stacked machine learning model

The response variable in the model is weekly egg abundance. Predictor variables consisted of lagged climatic and photoperiodic covariates selected to capture delayed mosquito responses to environmental conditions. Specifically, we included weekly median air temperature, weekly cumulative precipitation, and weekly median photoperiod, with each variable additionally having lagged rolling means ranging from 2 to 10 weeks.

We adopted a stacked ensemble learning approach, which integrates predictions from multiple base learners via a meta-learner to enhance accuracy and robustness (Wolpert 1992). Following the method implemented in Da Re et al. (2025), we used three base algorithms: XGBoost (Chen and Guestrin 2016), Random Forest (Breiman 2001), and Cubist (Kuhn et al. 2024).

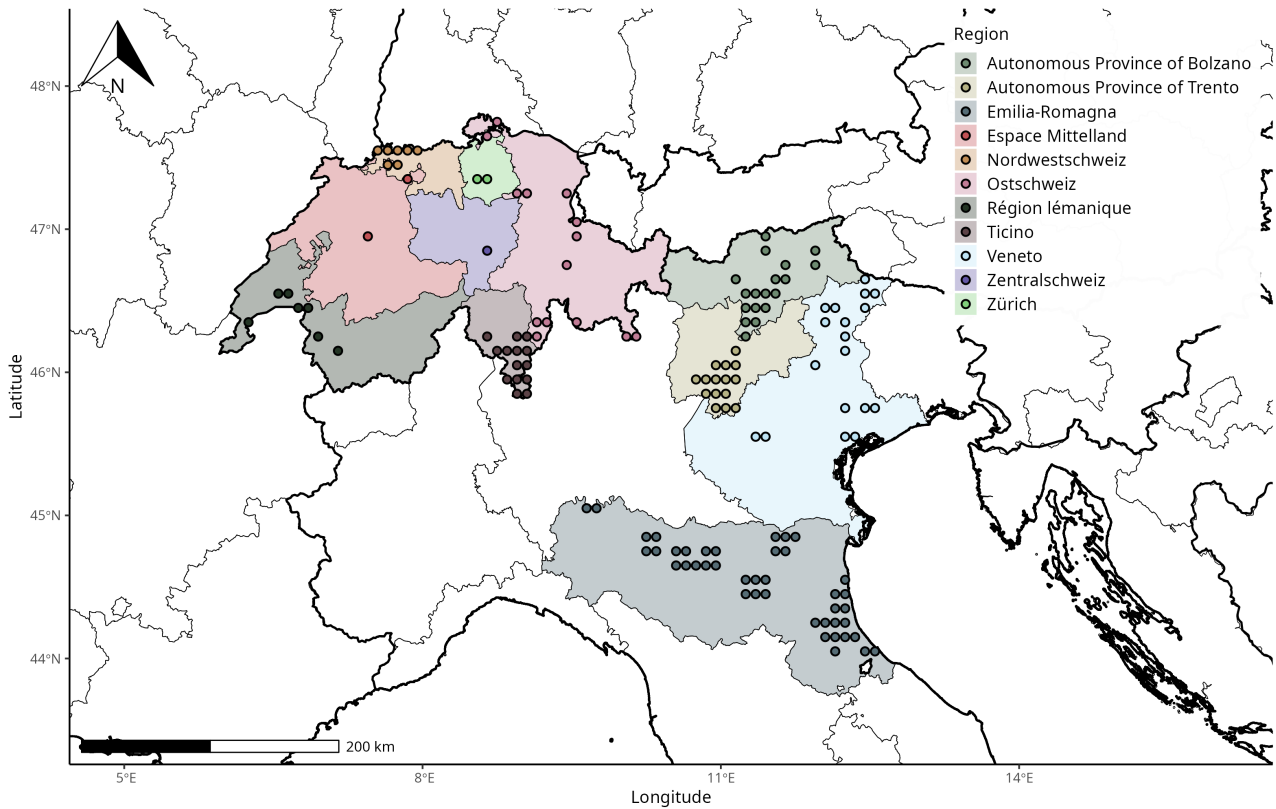


FIGURE 1 Geographic distribution of ovitrap observation locations after spatial aggregation. A total of 140 locations are represented across 11 administrative regions in Switzerland and northern Italy.

- **Random Forest** was implemented via the `ranger` library in R, which captures nonlinear interactions through ensembles of decision trees. Tuned hyperparameters were the number of trees, number of variables sampled at each split (`mtry`), and minimum node size.
- **Extreme Gradient Boosting (XGBoost)** fits boosted decision trees sequentially to minimize prediction error. Tuned hyperparameters included the number of boosting rounds, tree depth, learning rate, subsampling fraction, and column subsampling.
- **Cubist regression** is a rule-based model combining regression trees and linear models, tuned via the number of committees.

Hyperparameters for all base learners were optimised jointly using random search over predefined parameter spaces, with root mean squared error (RMSE) as the optimisation metric.

Predictions from the base algorithms were combined using a linear regression meta-learner. To avoid information leakage, base learner predictions were generated via internal cross-validation and only out-of-fold predictions were used to train the meta-learner. The stacked model was implemented using the `m1r3` and `m1r3pipelines` frameworks (Bischl et al. 2016, Lang et al. 2019).

To assess the relative contribution of predictors, variable importance was derived from the Random Forest component of the ensemble

using permutation-based importance scores. Importance values were normalised to percentages and grouped by predictor type (temperature, precipitation, photoperiod) and lag. The strongest predictors were lagged temperature variables, with the most importance consistently associated with intermediate lag windows (approximately 3–5 weeks), indicating a pronounced influence of thermal conditions on oviposition activity (Figure A2). Photoperiod and precipitation also contributed to model performance, although their relative importance in the model was lower.

2.3 | Model validation and projection

Before training, we partitioned the final dataset into spatially and temporally independent training and test sets to quantify predictive accuracy. Spatial validation was performed by withholding entire grid cells with ovitrap data from model training. Specifically, one grid cell was randomly selected within each region, conditional on the NUTS-2 region containing at least three distinct grid cells with ovitrap observations. This ensures sufficient spatial representation while providing a realistic assessment of the model's spatial generalisation capacity. To evaluate the model's performance under different climatic conditions than those used in training, we selected three climatically distinct years

(2012, 2014, 2022) from the 15-year record using a clustering-based exploratory analysis of temperature and precipitation anomalies (details in Appendix B). Two years represented extreme climatic conditions affecting *Ae. albopictus* phenology and abundance (Hawley 1988, Reinhold et al. 2018), while one was representative of average conditions, serving both as a baseline for model validation and as a representative reference of typical climatic conditions in the 2005–2024 period. 2012 exhibits an exceptionally warm and dry summer, coupled with a cold and dry winter; 2014 represents the opposite summer conditions, characterised by a cool and wet summer and a comparatively warm, wet winter; 2022 is classified by the algorithm as representative of average climatic conditions. This approach allows us to evaluate model performance under both current and future (unseen and/or more extreme) climate conditions.

Performance metrics included Root Mean Squared Error (RMSE) and coefficient of determination (R^2), computed separately for training, spatial, and temporal subsets. In addition, we calculated the Relative Root Mean Square Error (rRMSE), a dimensionless metric that expresses RMSE as a percentage of the observed data range. This normalisation accounts for the variability inherent in the observations, resulting in a scale-independent indicator of predictive accuracy. Values below 20% are generally interpreted as indicative of good predictive performance (Li et al. 2013, Despotovic et al. 2016, McGough et al. 2017), with model accuracy considered excellent when rRMSE < 10%.

Once validated, the trained model was applied to weekly climate covariates from 2005–2024, and predictions were averaged temporally to generate a baseline map of current abundance and distribution of *Ae. albopictus* oviposition activity.

2.4 | Future climate data

Future climate change data are based on the EURO-CORDEX community (Jacob et al. 2020) (the European branch of the World Climate Research Programme's Coordinated Regional Climate Downscaling Experiment), which offers ensembles of regional climate models (RCMs), generated by dynamically downscaling general circulation models (GCMs) from CMIP5 (Coupled Model Intercomparison Project Phase 5). Instead of using all emission scenarios (RCP2.6, 4.5, and 8.5, representative concentration pathways) and the full ensemble of RCMs (over 50 GCM-RCM combinations, number depending on scenario), we adopted an approach inspired by storyline climate scenarios that allows an easier interpretation of climate futures. Specifically, we selected from the RCP8.5 ensemble a sub-ensemble of three models that maximizes the range of expected changes thus offering interpretable climate futures based on physically consistent data.

We focused only on RCP8.5, which, despite its reduced likelihood, provides the strongest forcing signal and the largest ensemble spread, facilitating robust selection of contrasting narratives. Model selection relied on projected changes in summer and winter temperature and precipitation using the initialisation step of k-means clustering (Cannon 2015). For more details we refer to the supplementary material and to

the appendix of Napoli et al. (2026). Consequently, we use the term climate future instead of climate scenario, since we only used one RCP scenario but three different realisations from three different climate models.

Two projection periods were examined: mid-century (2036–2055) and late-century (2066–2085). Each period includes:

- (1) **Average change:** a baseline future representing ensemble-mean changes with average warming and limited seasonal precipitation shifts, implying slightly drier summers and slightly wetter winters.
- (2) **Warmer winters & wetter summers:** a warmer-wetter future characterised by warmer winters, and less warm and wetter summers.
- (3) **Warmer & drier summers:** a warmer-drier future with less warm winters and substantial summer drying that is accompanied by stronger warming.

Environmental datasets for the future periods were generated by adjusting the historical baseline (observations) with monthly climate change factors based on the RCM data. Future climate fields were generated using a change-factor (Δ) approach, in which statistically derived climate anomalies from regional climate models were applied to the observed E-OBS baseline. Daily E-OBS mean air temperature and precipitation fields were first cropped to the Alpine domain and retained at their native spatial and temporal resolution. Monthly change factors derived from EURO-CORDEX regional climate simulations were then applied to the E-OBS data in a variable-specific manner.

For temperature, change factors represented additive anomalies (in °C) relative to the historical reference period. These anomalies were spatially explicit and provided at a monthly resolution. Prior to application, temperature change-factor fields were resampled to the E-OBS grid using bilinear interpolation to ensure spatial congruence. The monthly temperature anomalies were then added to each corresponding daily E-OBS temperature field based on calendar month.

For precipitation, change factors were expressed as multiplicative ratios, reflecting relative changes in precipitation intensity. As for temperature, precipitation change-factor fields were resampled to the E-OBS grid. Monthly precipitation scaling factors were subsequently applied multiplicatively to the daily E-OBS precipitation fields according to month, preserving the temporal structure of observed precipitation variability while modifying its magnitude.

This procedure was repeated for two future time windows (2036–2055 and 2066–2085) and for three regional climate model realisations, each representing a distinct climate future within the same emission pathway. By construction, this change-factor approach preserves the observed spatial patterns, temporal sequencing, and interannual variability of the baseline climate, while superimposing physically consistent large-scale climate change signals derived from regional climate models. As such, it provides a robust and computationally efficient framework for generating future climate forcings suitable for impact modelling.

Moreover, it offers bias-adjusted future data, which is important for impact models, since RCMs can exhibit non-negligible biases (Matiu

et al. 2024). While this is a rather simplistic bias adjustment approach compared to, for example, quantile-based methods, our choice was motivated by the temporal constraints of the ovitrap data and the fact that the impact model needs to be trained on observations and cannot be trained on the historical period of climate models, which has no temporal synchrony to actual dates.

The ML model, trained on the observational dataset, was applied to the future climate datasets to generate predictions for each period and climate model. A schematic overview of the full data workflow is provided in Figure A1.

2.5 | Timing of seasonal activity

We quantified the timing of seasonal activity of *Ae. albopictus* in the Alps using the modelled weekly mosquito egg abundance. Weekly predictions were aggregated at the NUTS-2 level by averaging across all grid cells within each region.

The mosquito activity season was defined as the continuous sequence of weeks during which predicted egg abundance exceeded a minimum threshold, determined using the Period-Over-Threshold (POT) method (Da Re et al. 2025). Generalised additive models (GAMs) were fitted to predicted egg abundance as a function of time, and smoothed outputs were used to estimate onset and cessation of activity.

Region-specific seasonal patterns were characterised by fitting independent GAMs for each NUTS-2 region (Figure A3). For each region r weekly mean predicted abundance $y_{r,w}$ was modelled as:

$$y_{r,w} = \beta_0 + s_r(w) + \varepsilon_{r,w}, \quad (1)$$

where $y_{r,w}$ is the mean predicted egg abundance in week w , $s_r(\cdot)$ is a penalised regression spline over week, and $\varepsilon_{r,w}$ is the residual error. A basis dimension of $k = 15$ was used for the week smooth to allow flexibility to represent unimodal or weakly bimodal seasonal patterns, yet avoid overfitting of the curve.

For elevational GAMs, predicted egg abundance was also aggregated by week and 100 m elevation bands (Figure A4). A bivariate GAM was then fitted to the aggregated data according to:

$$y_{w,e} = \beta_0 + te(w, e) + \varepsilon_{w,e}, \quad (2)$$

where e denotes elevation (expressed as band midpoints) and $te(w, e)$ is a tensor-product smooth capturing potentially non-linear and non-additive interactions between seasonal timing and elevation. Basis dimensions were set to $k_w = 12$ for the temporal dimension and $k_e = 8$ for elevation.

All GAMs were fitted using restricted maximum likelihood (REML), which provides stable and unbiased estimation of smoothing parameters and is robust to overfitting, particularly in the presence of correlated temporal structure. Smoothed weekly predictions were generated on a regular grid (weeks 1–53, elevation midpoints), and negative fitted values were truncated at zero to ensure biological plausibility.

A fixed threshold corresponding to 5% of the overall maximum observed egg abundance was applied. Season onset and termination were defined as the first and last epidemiological weeks, respectively, during which the smoothed GAM predictions exceeded this threshold. For each combination of region (or elevation band), climate future, and time period, season length was calculated as the number of consecutive weeks above threshold.

3 | RESULTS

3.1 | Model performance evaluation

Model performance was assessed across training, spatial, and temporal test sets to evaluate goodness of fit, spatial transferability, and temporal generalisation. Observed versus predicted values for each data partition are shown in Figure 2, providing a visual assessment of model behaviour across contrasting validation contexts.

Within the training set, predicted values closely followed the 1:1 relationship across the full range of observed egg counts (Figure 2, left panel). The dense clustering of points along the identity line, combined with low dispersion, indicates that the model accurately captured non-linear relationships between environmental drivers and mosquito abundance (rRMSE = 1.73; $R^2 = 0.95$).

When evaluated on spatially independent test data, performance declined as expected but remained robust (rRMSE = 6.62; $R^2 = 0.55$). The spatial test panel (Figure 2, centre) shows increased scatter around the 1:1 line, particularly at higher observed values, reflecting genuine spatial heterogeneity and site-specific variability not encountered during training. Nevertheless, the model preserved the overall scaling of abundance and avoided systematic bias across low and intermediate egg counts, indicating meaningful spatial transferability.

Temporal validation exhibited greater dispersion (rRMSE = 6.23; $R^2 = 0.43$; Figure 2, right panel), consistent with the strong influence of inter-annual climatic variability on oviposition activity. In particular, extreme years showed broader spread and partial compression of predicted values at the upper tail of the distribution, suggesting reduced sensitivity to unusually high abundances under atypical climate conditions. This behaviour is consistent with conservative ensemble predictions and reflects the challenge of extrapolating to climatic combinations that differ substantially from the training period. Across individual years, predictive skill was highest under near-average climatic conditions (2022: rRMSE = 6.51; $R^2 = 0.54$) and lower during climatically extreme years (2012: warm, dry summer and cold winter; 2014: cool, wet summer), confirming that model uncertainty increases under environmental regimes approaching the limits of the observed climate space.

Overall, the observed–predicted relationships indicate that the model reliably captures broad spatio-temporal patterns in *Ae. albopictus* egg abundance, while appropriately expressing uncertainty under spatial extrapolation and climatic extremes. Variable importance analysis further supports the biological plausibility of the model, identifying

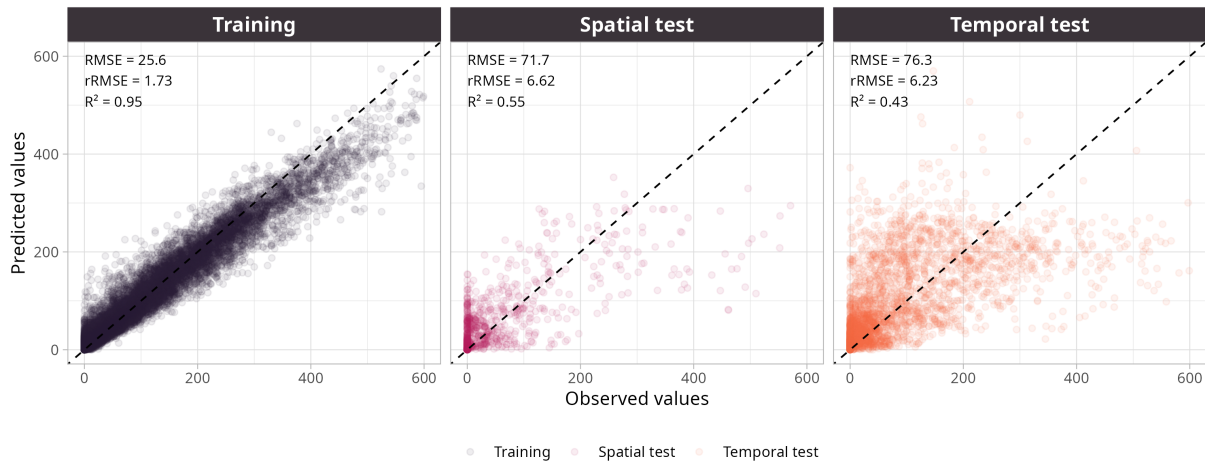


FIGURE 2 Observed versus predicted *Ae. albopictus* egg counts across training, spatial test, and temporal test partitions. Points represent weekly trap-level observations, and the 1:1 line indicates perfect agreement.

temperature, particularly the 4-week rolling mean, as the dominant predictor, followed by photoperiod and precipitation (Figure A2).

3.2 | Current abundance baseline

We reconstructed the spatio-temporal distribution of *Ae. albopictus* egg abundance by applying the trained model to weekly meteorological data for 2005–2024. The map (Figure 3a) displays predicted egg abundance per pixel averaged across the 20 years, representing contemporary baseline conditions. Spatially, high predicted egg abundances were concentrated in low-elevation plains and densely populated regions, particularly below 500–700 m a.s.l., while mountainous and forested areas exhibited consistently low values. Above approximately 1,500 m, predicted abundance was close to zero for most of the season.

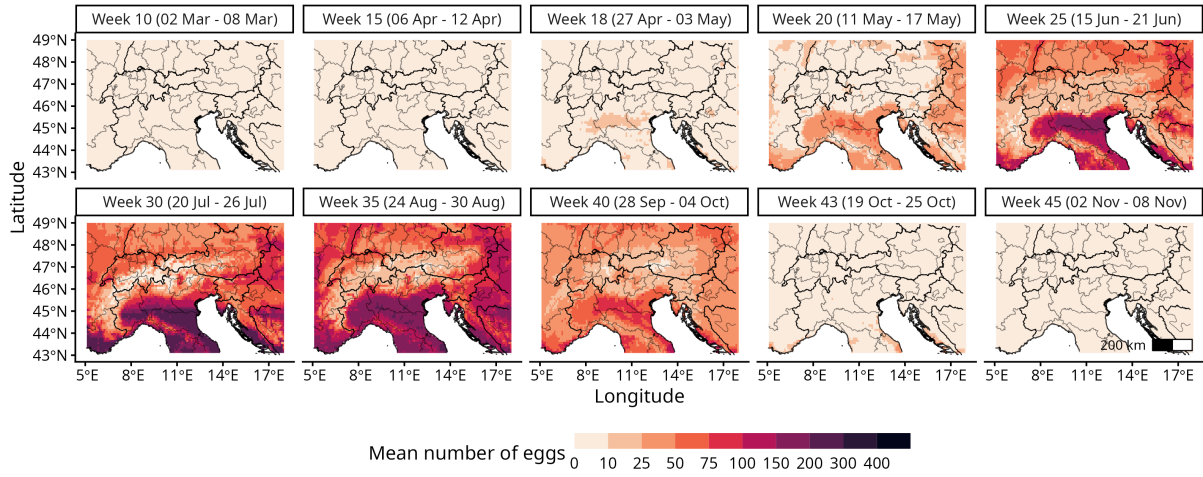
Temporally, egg abundance rose gradually in early spring, peaked mid-season, and declined toward autumn, consistent with known phenology of *Ae. albopictus*. Figure 3a shows a clear seasonal progression in space and time. During early spring (weeks 10–15), predicted oviposition activity was largely absent. From late April to early May (weeks 18–20), suitable conditions expanded rapidly across foothill regions, followed by widespread high abundances across low- and mid-elevation areas during summer (weeks 25–35). Peak spatial extent and intensity occurred between mid-June and late August, after which abundance declined rapidly, retreating to lowland regions by early November (week 45).

3.3 | Future abundance under different climates

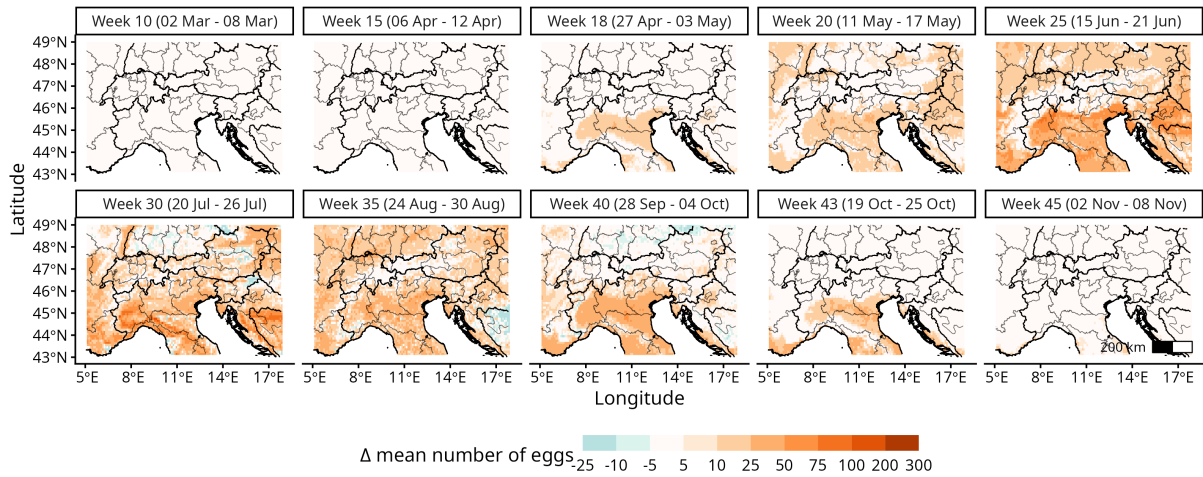
Future climate conditions are projected to intensify oviposition activity in already suitable lowland areas while simultaneously allowing substantial increases at higher elevations.

The model trained on present-day climate conditions and ovitrap observations was applied to future climate projections for the mid-century (2036–2055) and late-century (2066–2085) periods. Changes in egg abundance were quantified as the difference between future and current predictions (Δ , Delta), expressing projected changes relative to baseline. The spatial patterns of change under the 'average change' climate scenario are shown in Figures 3b–3c. Overall, the results reveal strongly spatially structured responses. Positive deltas are most consistently observed in lowland areas and major valleys, where populations are already established. In these regions, increases in predicted egg abundance are particularly pronounced from late spring through summer (approximately weeks 20–35), with local gains frequently exceeding +50 to +100 eggs per week per pixel and reaching even higher values in parts of northern Italy and the Alpine foreland. Moreover, projections indicate a progressive upward expansion of positive deltas into mid- and high-elevation areas. Although baseline predictions at higher elevations are close to zero for much of the year, future scenarios show increasingly widespread positive anomalies along valley flanks and lower mountain slopes, especially during the core summer period (e.g., weeks 25–35 in Figures 3b and 3c). These spatial patterns are largely consistent across climate futures, with inter-configuration differences primarily affecting the magnitude, and occasionally the sign, of mid-century changes rather than the overall spatial structure of the predicted response.

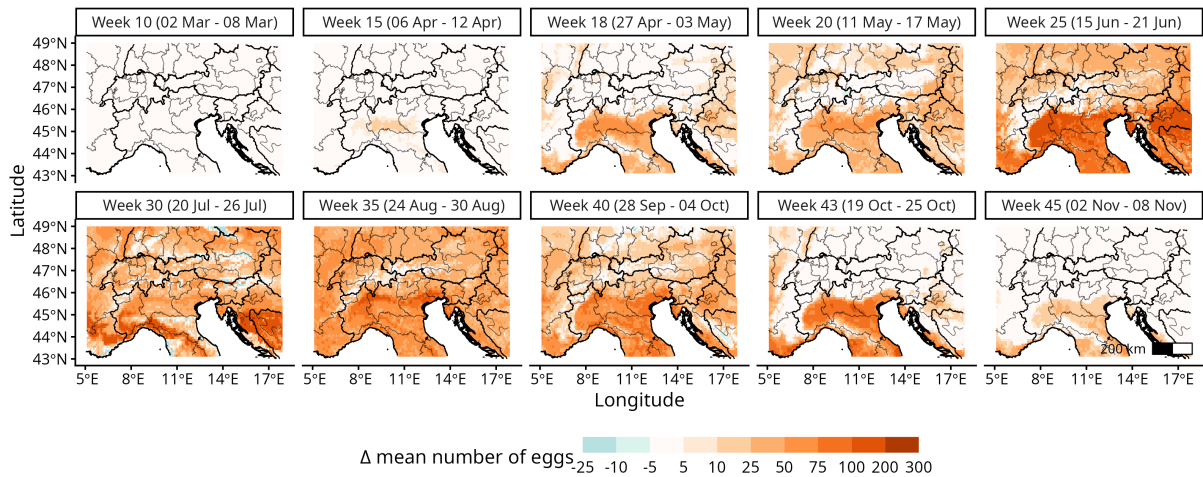
An exception is the mid-century warmer-winter and wetter-summer scenario (Figure A5a), which exhibits localised decreases in predicted egg abundance. These reductions are attributable to internal climate variability and the absence of net warming in this climate model for this period (Figure B9).



(a) Baseline mean predicted egg abundance (2005-2024).



(b) Change in predicted egg abundance during the mid-century (2036-2055) relative to the baseline.



(c) Change in predicted egg abundance during the late-century (2055-2086) relative to the baseline.

FIGURE 3 Spatial distribution of predicted *Ae. albopictus* egg abundance and temporal changes across the study area. Panel (a) shows the baseline mean predicted abundance averaged over 2005–2024. Panels (b) and (c) show average changes (Δ) in predicted abundance for the mid-century (2036–2055) and the late-century (2066–2085), respectively.

3.4 | Activity season

Seasonal curves of predicted mosquito abundance for the current baseline showed regional differences in timing and duration of activity across the Alpine study area (Figure A3). Italian regions with ovitraps mainly placed in the Po Valley (Veneto and Emilia-Romagna) generally exhibited earlier onset of activity (week 19) and later termination (week 43), resulting in longer predicted active seasons than most Swiss regions. Italian highly mountainous regions (Autonomous Province of Bolzano and Autonomous Province of Trento) and Swiss regions (Ostschweiz, Nordwestschweiz, Espace Mittelland, Zürich, Zentralschweiz, Région lémanique and Canton of Ticino) displayed slightly delayed onsets (weeks 22–23) and earlier terminations (weeks 41–42), indicating comparatively shorter seasonal windows.

Elevational effects on current seasonality were explicitly captured using two-dimensional GAMs (Figure A4a), and the fitted lines show a continuous gradient in both timing and magnitude of abundance across elevation. At lower elevations, the models predict earlier seasonal peaks and higher maximum abundance, while increasing elevation is associated with reduced peak magnitude, and compressed seasonal profiles.

Relative to the current baseline, the GAMs of the 'average change' configurations for both mid- and late-century in Figure A4 are progressively wider and more elevated, denoting a longer active season and increased abundance at higher altitudes in the future. Temporally, seasonal peaks widened and shifted later in the year, reflecting extended activity windows under future warming. Across the Alpine area, simulated mean season length increased from 18.8 ± 4.4 weeks (current) to 20.6 ± 3.8 weeks (mid-century average change) and 22.4 ± 3.7 weeks (late-century average change) (Table 1). Region-specific activity windows are reported in Table A2. The 'warmer winters & wetter summers' and 'warmer & drier summers' futures produced mean durations ranging between 18.7 and 22.1 weeks, confirming an overall extension of the modeled active period under all tested climate conditions. A modest exception is observed under the 'warmer winters & wetter summers' future for the mid-century period, where mean season length slightly decreases relative to the current baseline. The most pronounced increases occurred below 1500 m.

Temporal and altitudinal dynamics of these changes are further illustrated in Figure 4, which stratifies predicted delta abundances by week and elevation for climate future and period. Across all climate futures, earlier seasonal onset and higher peak abundance are evident at lower elevations, while higher-elevation sites show delayed and more moderate increases. The magnitude of these shifts is consistently weakest under the 'warmer winters & wetter summers' future (2), which exhibits the smallest deviations from present-day conditions. On the other hand, it is consistently higher for the 'warmer & drier summers' future, highlighting the strong influence of temperature changes on abundance.

4 | DISCUSSION

Climate warming is transforming the environmental boundaries of many vector species (Semenza and Paz 2021). In this study, we found that ongoing and projected warming substantially relaxes the climatic constraints limiting *Ae. albopictus* in mountainous environments, enabling both upslope expansion and pronounced increases in abundance at higher elevations. These findings are consistent with previous work documenting the rapid establishment and continued spread of this invasive species across southern Europe (Dalla Pozza and Majori 1992, Tisseuil et al. 2018, Romiti et al. 2021), as well as its accelerated northward colonisation into central and western Europe, including France and more northern regions (Radici et al. 2025, Farooq et al. 2025).

The Alpine arc, characterised by steep climatic gradients and densely populated foothills, provides a natural laboratory for examining how environmental conditions jointly shape the dynamics of climate-sensitive vectors such as *Ae. albopictus*. Assessing the species' potential to expand into cooler, high-elevation environments under climate change is therefore a necessary step for anticipating future nuisance levels and the risk of autochthonous arbovirus transmission in previously unaffected regions (Laverdeur et al. 2024).

Contextualising our projections within climate warming in the Alps is fundamental for interpreting the results obtained. High mountains and high latitudes are recognised as experiencing some of the strongest warming trends globally (IPCC 2021, C3S 2024). This phenomenon, commonly referred to as 'elevation-dependent warming' or 'mountain amplification', leads to faster temperature increases in mountainous regions compared to adjacent lowlands (Pepin et al. 2022). Such accelerated warming directly contributes to the relaxation of the thermal limits constraining *Ae. albopictus* (McCain and Garfinkel 2021), thereby driving the predicted upslope expansion and the substantial increases in egg abundance.

4.1 | Model performance, robustness, and limitations

The predictive performance of our modelling framework supports its robustness and applicability for assessing climate-driven changes in *Ae. albopictus* dynamics across complex mountain landscapes. The model retained predictive skill when extrapolated to previously unseen locations and climatically distinct years (Figure 2), indicating that it learned generalisable relationships between mosquito dynamics and environmental drivers rather than site-specific artefacts.

The dominant contribution of temperature and photoperiod to model performance is biologically well founded. Both variables are primary regulators of mosquito development, survival, and diapause timing (Hawley 1988, Delatte et al. 2009, Reinhold et al. 2018), and their consistent ranking at the top of the variable-importance (Figure A2) analysis demonstrates that the model is structured around ecologically meaningful drivers. Machine-learning models infer predictive structure

TABLE 1 Mean (\pm SD, standard deviation) of simulated *Ae. albopictus* season length (weeks) under current and future climate across the Alps and their surroundings.

Period and climate future	Mean season length (weeks \pm SD)
2005–2024	
Current period	18.8 \pm 4.4
2036–2055	
(1) Average change	20.6 \pm 3.8
(2) Warmer winters & wetter summers	18.7 \pm 3.9
(3) Warmer & drier summers	19.8 \pm 4.0
2066–2085	
(1) Average change	22.4 \pm 3.7
(2) Warmer winters & wetter summers	20.8 \pm 3.6
(3) Warmer & drier summers	22.1 \pm 3.2

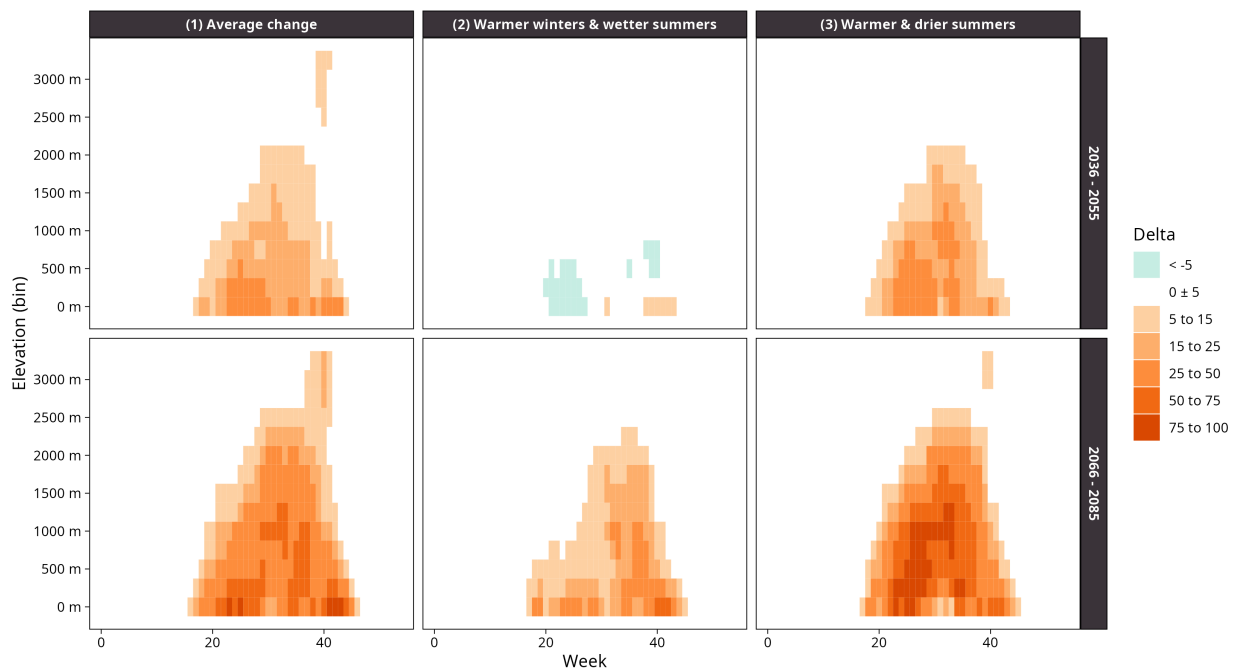


FIGURE 4 Hovmöller diagrams depicting changes (Δ , Delta) in simulated *Ae. albopictus* abundances across elevation bins of 250 m and weeks of the year, derived by subtracting current predictions (2005–2024) from each of the climate future and periods.

directly from data through the optimisation of complex, non-linear relationships, and their interpretability therefore rests on whether the learned feature hierarchy is consistent with established biological mechanisms. In this case, the ranking of predictors is fully coherent with physiological knowledge, with temperature and photoperiod emerging as the dominant controls of development, survival, and diapause regulation in *Ae. albopictus*. This concordance provides strong evidence that the model has internalised the causal climatic constraints governing population dynamics, rather than relying on coincidental correlations, a property increasingly recognised in ecological applications of machine learning when models are trained on mechanistically relevant covariates (Dormann et al. 2018, Molnar 2019, Pichler and Hartig 2023).

Nevertheless, several limitations define the scope within which our projections should be interpreted. The model is trained on ovitrap-derived egg counts, which provide a sensitive index of reproductive activity but do not directly represent adult abundance or vectorial capacity. While egg abundance is strongly correlated with local population dynamics (Da Re et al. 2024), translating these patterns into epidemiological risk requires additional assumptions. Moreover, by design, the model isolates climatic drivers and does not explicitly account for land use, urbanisation, or human-mediated dispersal, all of which are known to modulate *Ae. albopictus* establishment at fine spatial scales (Li et al. 2014, Westby et al. 2021). This is further explored in section 4.3.

Moreover, our model does not explicitly account for spatially and temporally heterogeneous vector control interventions, which can locally suppress oviposition independently of climatic suitability. Vector

control may reduce absolute egg abundance, and future integration of control intensity data could improve the accuracy of the model. In addition, ovitrap egg counts are effectively set to zero during the winter months under current climatic conditions. This reflects standard surveillance practice, where monitoring is not carried out during winter months, and the seasonal diapause of *Ae. albopictus* at low temperatures (Hawley 1988, Delatte et al. 2009). Incorporating data from winter monitoring could significantly enhance model performance, because if low-level oviposition occurs during mild winters and remains undetected, this assumption could lead to a conservative bias in current egg abundance estimates. Under future warming scenarios, such a bias would likely result in an underestimation of early-season activity and the degree of winter carry-over, thereby dampening projected advances in season onset and total season length. Consequently, our projections of warming-induced phenological extension should be interpreted as lower-bound estimates. Projected warming, particularly milder winters, could favour the emergence of non-diapausing populations, leading to a more continuous seasonal activity than currently simulated. Empirical evidence from the Mediterranean Basin indicates that continuous oviposition has already been observed in Italy (Bonacci et al. 2015), suggesting that diapause suppression may represent an adaptive response to warming, potentially driven by selection for longer activity periods and reduced diapause costs (Lacour 2016).

Uncertainty also arises when projecting under future climates that increasingly depart from historical conditions. Although ensemble learning and storyline-based climate selection reduce sensitivity to individual model biases, extrapolation beyond the observed climate envelope inevitably introduces uncertainty (Thuiller et al. 2019). Importantly, this uncertainty primarily affects the magnitude of predicted abundance rather than the direction of change. The consistent signal of upslope expansion and seasonal extension across all climate futures indicates that these qualitative trends are robust to modelling assumptions.

Our model predicts that *Ae. albopictus* egg abundance in the Alps will increase substantially by mid-century and even more intensively by late-century. The projected upslope expansion aligns with widespread elevational range shifts observed in numerous montane insect taxa. As noted by McCain and Garfinkel (2021), warming typically drives upward movement of both lower and upper range limits, but responses can vary depending on life-history traits, microclimate, and the strength of non-thermal niche components such as precipitation and humidity. *Ae. albopictus* has a lower developmental threshold of roughly 10–12 °C, an optimal performance near 28–30 °C, and steep declines in survival above 32–35 °C (Delatte et al. 2009, Reinhold et al. 2018, Marini et al. 2020). In our predictions, the species' expansion into higher elevations reflects the expected response to a progressive relaxation of thermal constraints; these are an upward displacement of the climatic envelope that currently limits persistence at altitude. However, as McCain and Garfinkel (2021) emphasises, early phases of climate-driven expansion often produce asymmetric range shifts, wherein the upper limit advances while the lower limit remains relatively stable. This pattern could apply to *Ae. albopictus*, whose foothill populations likely act

as sources for recurrent colonisation of newly suitable high-elevation sites.

Regional disparities in predicted change are also informative, such as the limited response in regions of the Po Valley (Figure A3), which may reflect ecological saturation where current climatic conditions already support near-maximal population levels. Similar patterns have been modelled for southern Italian regions, where extreme summer temperatures increasingly exceed thermal optima and suppress further growth (Radici et al. 2025). Experimental evidence shows that population growth rates of *Ae. albopictus* increase with temperature, as higher thermal regimes accelerate larval development and adult emergence, yielding greater intrinsic rates of increase (r) (Alto and Juliano 2001, Huxley et al. 2021, Garrido Zornoza et al. 2024). This mechanistic link supports our model's projection of faster seasonal population buildup and higher egg abundance under warming scenarios, particularly in pre-mountain areas where current temperatures still constrain development. Beyond simple mean temperature, future adaptation by mosquitoes may also involve the adaptive evolution of thermal tolerance or shifts in plastic responses (Couper et al. 2021), which could further enable the species' persistence and expansion under a changing climate.

Another study by Reinhold et al. (2018) shows that rising spring temperatures can speed up larval development and adult emergence, while delayed autumn cooling postpones the onset of diapause induction. Consistent with this, Parmesan (2006) reported that even species with photoperiodically regulated phenology have responded to temperature-driven selection, advancing their spring activity or extending it into the fall. Our results reflect these same mechanisms, with model projections indicating both earlier seasonal onset and delayed termination of oviposition, particularly under late-century warming.

Temperature has been long identified as the most important abiotic factor affecting the life of poikilotherms like mosquitoes, influencing their development, survival, and adult activities like flight and host-seeking behaviour. Indeed, studies aimed at identifying new areas of potential invasion, usually consider temperature as one of the main predictors (Caminade et al. 2012, Fischer et al. 2014, Kraemer et al. 2019, Neteler et al. 2011, Marini et al. 2020), which aligns with our model's variable importance, which had temperature as the most important variable.

The predicted shifts extend the window of reproductive activity by more than three weeks until late-century, especially in pre-mountain and mid-elevation areas. Comparable climate-driven phenological shifts have been observed across a range of ectothermic taxa, suggesting that the prolongation of *Ae. albopictus* seasonal activity we project is part of a broader biological trend. For instance, recent warming in East Asia has advanced spring onset and delayed autumn cooling, resulting in an extended activity period and northward expansion of the Asian mantis *Hierodula patellifera* (Shin et al. 2023). This study documented hatching up to two months earlier and adult activity persisting nearly one month later than historical records, directly linked to warmer spring and autumn temperatures.

Taken together, these independent observations reinforce the hypothesis of a future season lengthening and elevational expansion, as predicted by our model for *Ae. albopictus*.

4.2 | Cold tolerance, adaptation, and expansion into cold mountain environments

Recent advances in evolutionary and molecular ecology further support the biological plausibility of the upslope expansion projected in our study. Although *Ae. albopictus* originates as a sub-tropical and tropical species, multiple lines of evidence indicate a substantial capacity for cold tolerance and local adaptation across its native and invaded ranges. Comparative studies on the native Asian range demonstrate pronounced differentiation in overwintering survival, diapause intensity, and thermal performance, suggesting that cold adaptation has evolved repeatedly in response to regional climatic constraints (Kramer et al. 2021).

Genomic and transcriptomic analyses have identified selection acting on pathways related to energy metabolism, membrane stability, and stress response in populations exposed to colder climates, indicating that low-temperature tolerance is based on heritable mechanisms rather than phenotypic plasticity alone (Sherpa et al. 2019 2022). Experimental work further shows that cold-acclimated populations exhibit higher egg survival, improved diapause performance, and enhanced post-winter fitness compared with populations from warmer regions (Sherpa et al. 2022). Together, these findings suggest that *Ae. albopictus* possesses both the physiological and evolutionary capacity to persist under increasingly cold and seasonal environments.

Evidence from high-elevation systems reinforces this interpretation. Several studies have documented the presence and establishment of *Aedes* species, including *Ae. albopictus* and closely related taxa, in mountainous regions of the Himalaya, where populations persist under low winter temperatures, short growing seasons, and strong climatic seasonality (Sherpa et al. 2019, Phuyal et al. 2020, Dhimal et al. 2021, Kramer et al. 2023). These findings demonstrate that steep elevational gradients do not represent absolute barriers to colonisation once minimum thermal thresholds are exceeded, particularly when seasonal windows of activity are sufficiently long to allow completion of the life cycle.

Within this broader context, our projections of upward range expansion in the Alps are consistent with both evolutionary evidence and real-world observations from other mountain systems. As mentioned, warming temperatures are likely to relax the primary abiotic constraint limiting persistence at altitude, while existing cold-adapted traits and standing genetic variation may facilitate rapid adjustment to newly suitable environments. Importantly, this implies that projected expansion is unlikely to be transient, but may instead result in stable seasonal populations capable of long-term persistence, particularly where climatic suitability intersects with anthropogenic habitat availability.

4.3 | Climatic vs. anthropogenic controls on expansion

In this study, our modelling approach intentionally isolated climatic drivers (temperature, precipitation, photoperiod) to quantify the direct influence of climate change on physiological and phenological constraints, thereby providing a clear estimate of its potential altitudinal and temporal expansion under future thermal regimes.

Nevertheless, climate change operates across multiple, interconnected dimensions that transcend disciplinary boundaries, as human societies, ecosystems, and the climate system are tightly coupled through complex feedbacks (Jebeile and Roussos 2023). As a result, climatic suitability alone cannot explain the full dynamics of *Ae. albopictus*' invasion. Rather, the species' spread emerges from a multifactorial socio-ecological process in which climate warming creates the environmental opportunity space, while human-mediated factors ultimately shape the likelihood, pathways, and long-term persistence of colonisation. Although temperature emerges as the principal enabling factor for upslope expansion, *Ae. albopictus* exhibits a marked affinity for anthropised habitats, making human presence and behaviour strong non-climatic determinants of establishment. Numerous studies have shown that urbanisation, human mobility, and the availability of artificial container habitats fundamentally shape its distribution at fine scales (Li et al. 2014, Manica et al. 2016, Westby et al. 2021, Torina et al. 2023). Breeding success relies heavily on man-made water containers, and transport networks facilitate both passive dispersal of eggs and repeated reintroductions, allowing otherwise marginal populations to persist.

Empirical evidence from Italy already demonstrates the species' capacity to colonise higher elevations than previously expected. Stable populations have been documented up to 900 m in the Lazio region (Romiti et al. 2022), with additional records showing persistent colonisation of mountain areas above 600 m a.s.l. in the surroundings of Trento city, northeastern Italy (Battistin et al. 2024). These observations indicate that in situ ecological constraints may be more permissive than historical records suggested and that the species has already overcome previously assumed altitude limits in multiple Italian mountain areas. This pattern is consistent with broader insights from invasion ecology: once minimum thermal thresholds are met, propagule pressure and habitat provisioning by humans become decisive drivers of establishment success.

Looking ahead, socio-economic trends may further reinforce upslope movement. Climate change is projected to alter the attractiveness and usability of Alpine landscapes, with substantial implications for mountain tourism (Steiger et al. 2024). Warmer summers in foothill and valley zones are expected to shift recreational and residential activity towards higher elevations, increasing human presence and infrastructure in areas that are concurrently becoming thermally suitable for *Ae. albopictus*. At the same time, broader demographic pressures, such as Europe's ageing populations and labour shortages, are likely to stimulate new development, seasonal mobility, and investment in upland tourism

economies (Harper 2013). Collectively, these processes expand anthropogenic container habitat availability and increase opportunities for human mediated dispersal, amplifying colonisation risks independently of climate.

Specifically, this intensification of human activity at newly suitable elevations, whether through permanent relocation, second-home development, or tourism, creates precisely the type of artificial container habitat that *Ae. albopictus* exploits for breeding. Increased residential infrastructure, water storage, and outdoor amenities expand the availability of oviposition sites, thereby facilitating both the establishment and long-term persistence of populations once thermal constraints are removed. Furthermore, greater human mobility within mountain regions amplifies the opportunities for passive mosquito dispersal. *Ae. albopictus* is a highly effective "stowaway", and human-assisted transport remains the dominant mechanism of long-distance spread (Tatem et al. 2006, Eritja et al. 2017). Upslope flows of goods, vehicles, and people can therefore seed newly suitable high-elevation habitats with repeated introductions, transforming areas that would otherwise remain marginal into established targets of colonisation.

Thus, these socio-economic facets of climate adaptation and mobility have the potential to accelerate the change in the biological range of *Ae. albopictus*, reinforcing the coupling between the climatic and anthropogenic drivers. Anticipating future vector distributions in the Alps and their surroundings will require surveillance and control strategies that explicitly integrate both dimensions.

Furthermore, the continued expansion of *Ae. albopictus* carries substantial economic implications. Invasive species globally generate damages an order of magnitude greater than the funds allocated for their management, with damage costs rising twice as rapidly as management expenditures (Diagne et al. 2021). This persistent imbalance reflects chronic underinvestment in prevention and early detection, despite strong evidence that proactive measures are far more cost-effective than reactive interventions (for example, Holden et al. 2016). For *Ae. albopictus*, the financial burden of emergency vector control and outbreak response substantially exceeds that of sustained monitoring and targeted containment (Roiz et al. 2024). These trends call for coordinated, cross-border frameworks in transalpine regions, where ecological and human connectivity transcend national boundaries. Coordinating resources between countries and aligning climate adaptation with vector-control policy could substantially mitigate both financial and health impacts. As with other invasive species, proactive and evidence-driven management, backed by consistent funding and international collaboration, will be essential to mitigate the rising economic impacts of biological invasions in a changing climate (Diagne et al. 2021).

5 | CONCLUSIONS

Our findings demonstrate that climate change will reshape the spatial and temporal dynamics of *Ae. albopictus* in the Alps and provide the first spatio-temporal projections of this invasive vector across a major

European mountain system. By integrating long-term surveillance data with climate data using machine-learning models, we show that ongoing warming is likely to expand climatically suitable conditions toward higher elevations and to substantially lengthen the seasonal window of mosquito activity. These changes redefine the Alps, from a historical barrier to invasion, into an emerging landscape of vector establishment and persistence. Mountain regions should therefore be recognised as frontiers for future mosquito colonisation and potential disease risk, requiring early, climate-informed surveillance and coordinated cross-border management under continued global warming.

AUTHOR CONTRIBUTIONS

Margo Blaha led the study by conceiving the research, developing the methodology, and coordinating the overall workflow. She performed the data curation, and validation, carried out the formal analyses, and developed the modelling component. She also interpreted the results and led the writing of the original draft and subsequent revisions. Michael Matiu contributed to the conceptualisation of the study and the development of the climate scenarios, including the analysis and processing of climate data, and contributed to writing and revising the manuscript. Bruno Majone and Dino Zardi contributed to the conceptualisation of the study, to the development of the methodological framework for the climate scenarios, to the validation of the modelling framework, and participated in the revision of the manuscript. Eleonora Flacio and Nikolaeta Anicic provided and curated the Swiss entomological surveillance data that were collected and prepared by the different teams of the Swiss Mosquito Network. Different field teams, including the Swiss Mosquito Network, collected the data. Annapaola Rizzoli provided the entomological data from the Autonomous Province of Trento, while Alberta Stenico and Filippo Cassina provided the entomological data from the Autonomous Province of Bolzano (South Tyrol). Roberto Rosà contributed to the conceptualisation and methodological development of the study, supervised the research, and contributed to the interpretation of the results and manuscript revisions. Daniele Da Re contributed to the conceptualisation and methodological development of the study, supported data integration and investigation activities, provided resources, and supervised the research. All authors contributed to the review and editing of the manuscript and approved the final version.

ACKNOWLEDGMENTS

We thank all regional and local surveillance teams involved in ovitrap monitoring for their sustained efforts in data collection over multiple years. We are grateful to the institutions and public health authorities in Italy and Switzerland for facilitating access to entomological datasets and supporting long-term mosquito surveillance activities. We also thank colleagues who provided constructive feedback during the development of this work.

SWISS MOSQUITO NETWORK

Gabi Müller, City of Zurich, Urban Pest Advisory Service, Switzerland.

Email: gabi.mueller@zuerich.ch

Daniel Cherix, University of Lausanne, Lausanne, Switzerland.

Email: daniel.cherix@unil.ch

Martin Gschwind, Swiss Tropical and Public Health Institute, Allschwil, Switzerland AND University of Basel, Basel, Switzerland.

Email: Martin.Gschwind@swisstph.ch

Bianca Modespacher, Swiss Tropical and Public Health Institute, Allschwil, Switzerland AND University of Basel, Basel, Switzerland.

Email: Bianca.Modespacher@swisstph.ch

Pie Müller, Swiss Tropical and Public Health Institute, Allschwil, Switzerland AND University of Basel, Basel, Switzerland.

Email: Pie.Mueller@swisstph.ch

Klaudia Erndle, University of Applied Sciences and Arts of Southern Switzerland, Mendrisio, Switzerland.

Email: klaudia.erndle@supsi.ch

FINANCIAL DISCLOSURE

The authors report no financial interests or potential conflicts of interest related to this study.

CONFLICT OF INTEREST

The authors declare no potential conflict of interests.

REFERENCES

- Adhami, J. & Reiter, P. (1998) Introduction and establishment of *aedes (stegomyia) albopictus* skuse (diptera: Culicidae) in albania. *Journal of the American Mosquito Control Association*, 14(3), 340–343.
- Alto, B.W. & Juliano, S.A. (2001) Temperature effects on the dynamics of *aedes albopictus* (diptera: Culicidae) populations in the laboratory. *Journal of medical entomology*, 38(4), 548–556.
- Battistin, G., Franceschini, A., Paoli, F. & Lencioni, V. (2024) Colonization by tiger mosquito (*aedes albopictus* skuse, 1894) of mountain areas over 600 m above sea level in the surroundings of trento city, northeast italy. *Journal of Entomological and Acarological Research*, 56(1).
- Bischi, B., Lang, M., Kotthoff, L., Schiffrer, J., Richter, J., Studerus, E. et al. (2016) mlr: Machine learning in r. *Journal of Machine Learning Research*, 17(170), 1–5.
- Boé, J., Somot, S., Corre, L. & Nabat, P. (2020) Large discrepancies in summer climate change over europe as projected by global and regional climate models: causes and consequences. *Climate Dynamics*, 54, 2981–3002.
- Bohers, C., Vazeille, M., Bernaoui, L., Pascalin, L., Meignan, K., Mousson, L. et al. (2024) *Aedes albopictus* is a competent vector of five arboviruses affecting human health, greater paris, france, 2023. *Eurosurveillance*, 29(20), 2400271.
- Bonaccini, T., Mazzei, A., Hristova, V.K. & Ahmad, M.A. (2015) Monitoring of *aedes albopictus* (diptera, culicidae) in calabria, southern italy. *International Journal of Scientific & Engineering Research*, 6(5), 1186–89.
- Breiman, L. (2001) Random forests. *Machine learning*, 45, 5–32.
- C3S (2024) *European state of the climate 2023*. Online report. URL https://climate.copernicus.eu/sites/default/files/custom-uploads/ESOTC%202023/Summary_ESOTC2023.pdf
- Cahill, A.E., Aiello-Lammens, M.E., Caitlin Fisher-Reid, M., Hua, X., Karanewsky, C.J., Ryu, H.Y. et al. (2014) Causes of warm-edge range limits: systematic review, proximate factors and implications for climate change. *Journal of Biogeography*, 41(3), 429–442.
- Caminade, C., Medlock, J.M., Ducheyne, E., McIntyre, K.M., Leach, S., Baylis, M. et al. (2012) Suitability of european climate for the asian tiger mosquito *aedes albopictus*: recent trends and future scenarios. *Journal of the Royal Society Interface*, 9(75), 2708–2717.
- Cannon, A.J. (2015) Selecting GCM Scenarios that Span the Range of Changes in a Multimodel Ensemble: Application to CMIP5 Climate Extremes Indices. *Journal of Climate*, 28(3), 1260–1267. doi:10.1175/JCLI-D-14-00636.1, publisher: American Meteorological Society Section: Journal of Climate. URL <https://journals.ametsoc.org/view/journals/clim/28/3/jcli-d-14-00636.1.xml>
- Chen, T. & Guestrin, C. Xgboost: A scalable tree boosting system. In: *Proceedings of the 22nd acm sigkdd international conference on knowledge discovery and data mining*, 2016, pp. 785–794.
- Coppola, E., Nogherotto, R., Ciarlo, J.M., Giorgi, F., van Meijgaard, E., Kadyrov, N. et al. (2021) Assessment of the european climate projections as simulated by the large euro-cordex regional and global climate model ensemble. *Journal of Geophysical Research: Atmospheres*, 126(4), e2019JD032356. doi:<https://doi.org/10.1029/2019JD032356>, e2019JD032356. URL <https://agupubs.onlinelibrary.wiley.com/doi/abs/10.1029/2019JD032356>
- Cornes, R.C., Van Der Schrier, G., Van Den Besselaar, E.J. & Jones, P.D. (2018) An ensemble version of the e-obs temperature and precipitation data sets. *Journal of Geophysical Research: Atmospheres*, 123(17), 9391–9409.
- Couper, L.I., Farner, J.E., Caldwell, J.M., Childs, M.L., Harris, M.J., Kirk, D.G. et al. (2021) How will mosquitoes adapt to climate warming? *elife*, 10, e69630.
- Da Re, D., Marini, G., Bonannella, C., Laurini, F., Manica, M., Anicic, N. et al. (2025) Modelling the seasonal dynamics of *aedes albopictus* populations using a spatio-temporal stacked machine learning model. *Scientific Reports*, 15(1), 3750.
- Da Re, D., Marini, G., Bonannella, C., Laurini, F., Manica, M., Anicic, N. et al. (2024) Vectabundance: a spatio-temporal database of *aedes* mosquitoes observations. *Scientific Data*, 11(1), 636.
- Da Re, D., Van Bortel, W., Reuss, F., Müller, R., Boyer, S., Montarsi, F. et al. (2022) dynamo: a unified modelling framework for invasive *aedes* mosquitoes. *Parasites & vectors*, 15(1), 414.
- Dalla Pozza, G. & Majori, G. (1992) First record of *aedes albopictus* establishment in italy. *Journal of the American Mosquito Control Association*, 8(3), 318–320.
- Delatte, H., Gimonneau, G., Triboire, A. & Fontenille, D. (2009) Influence of temperature on immature development, survival, longevity, fecundity, and gonotrophic cycles of *aedes albopictus*, vector of chikungunya and dengue in the indian ocean. *Journal of medical entomology*, 46(1), 33–41.
- Despotovic, M., Nedic, V., Despotovic, D. & Cvetanovic, S. (2016) Evaluation of empirical models for predicting monthly mean horizontal diffuse solar radiation. *Renewable and Sustainable Energy Reviews*, 56, 246–260.
- Dhimal, M., Kramer, I.M., Phuyal, P., Budhathoki, S.S., Hartke, J., Ahrens, B. et al. (2021) Climate change and its association with the expansion of vectors and vector-borne diseases in the hindu kush himalayan region: A systematic synthesis of the literature. *Advances in Climate Change Research*, 12(3), 421–429.
- Diagne, C., Leroy, B., Vaissière, A.C., Gozlan, R.E., Roiz, D., Jarić, I. et al. (2021) High and rising economic costs of biological invasions worldwide. *Nature*, 592(7855), 571–576.
- Dormann, C.F., Bobrowski, M., Dehling, D.M., Harris, D.J., Hartig, F., Lischke, H. et al. (2018) Biotic interactions in species distribution modelling: 10 questions to guide interpretation and avoid false conclusions. *Global ecology and biogeography*, 27(9), 1004–1016.
- Dumont, M., Monteiro, D., Filhol, S., Gascoin, S., Marty, C., Hagenmuller, P. et al. (2025) The european alps in a changing climate: physical trends and impacts. *COMPTES RENDUS GEOSCIENCE*, 357. doi:10.5802/crgeos.288.
- Eritja, R., Palmer, J.R., Roiz, D., Sanpera-Calbet, I. & Bartumeus, F. (2017) Direct evidence of adult *aedes albopictus* dispersal by car. *Scientific reports*, 7(1), 14399.

- Farooq, Z., Rocklöv, J. & Semenza, J.C. (2025) Northward expansion of aedes albopictus-associated arbovirus transmission risk in Europe. *The Lancet Planetary Health*.
- Ferraguti, M., Magallanes, S. & Ibáñez-Justicia, A. (2022) 8. Implication of human landscape transformation on mosquito populations. In: *Ecology of diseases transmitted by mosquitoes to wildlife* Wageningen Academic, pp. 143–160.
- Fischer, D., Thomas, S.M., Neteler, M., Tjaden, N. & Beierkuhnlein, C. (2014) Climatic suitability of aedes albopictus in Europe referring to climate change projections: comparison of mechanistic and correlative niche modelling approaches. *Eurosurveillance*, 19(6), 1–13.
- Flacio, E., Engeler, L., Tonolla, M. & Müller, P. (2016) Spread and establishment of aedes albopictus in southern Switzerland between 2003 and 2014: an analysis of oviposition data and weather conditions. *Parasites & Vectors*, 9(1), 304.
- Focks, D.A. et al. (2004) A review of entomological sampling methods and indicators for dengue vectors.
- Garrido Zornoza, M., Caminade, C. & Tompkins, A.M. (2024) The effect of climate change and temperature extremes on aedes albopictus populations: a regional case study for Italy. *Journal of The Royal Society Interface*, 21(220), 20240319.
- Giunti, G., Becker, N. & Benelli, G. (2023) Invasive mosquito vectors in Europe: From bioecology to surveillance and management. *Acta Tropica*, 239, 106832.
- Gobiet, A., Kotlarski, S., Beniston, M., Heinrich, G., Rajczak, J. & Stoffel, M. (2014) 21st century climate change in the European Alps—a review. *Science of the total environment*, 493, 1138–1151.
- Hanson, S.M. & Craig Jr, G.B. (1994) Cold acclimation, diapause, and geographic origin affect cold hardiness in eggs of aedes albopictus (Diptera: Culicidae). *Journal of medical entomology*, 31(2), 192–201.
- Harper, S. (2013) Population–environment interactions: European migration, population composition and climate change. *Environmental and Resource Economics*, 55(4), 525–541.
- Hawley, W.A. (1988) The biology of aedes albopictus. *Journal of the American Mosquito Control Association. Supplement*, 1, 1–39.
- Hock, R., Rasul, G., Adler, C., Cáceres, B., Gruber, S., Hirabayashi, Y. et al. (2019) High mountain areas. In: *IPCC special report on the ocean and cryosphere in a changing climate* H.-O. Pörtner, DC Roberts, V. Masson-Delmotte, P. Zhai, M. Tignor, E. ..., pp. 131–202.
- Holden, M.H., Nyrop, J.P. & Ellner, S.P. (2016) The economic benefit of time-varying surveillance effort for invasive species management. *Journal of Applied Ecology*, 53(3), 712–721.
- Huxley, P.J., Murray, K.A., Pawar, S. & Cator, L.J. (2021) The effect of resource limitation on the temperature dependence of mosquito population fitness. *Proceedings of the Royal Society B*, 288(1949), 20203217.
- IPCC (2021) *Climate Change 2021: The Physical Science Basis*. Cambridge, UK and New York, NY, USA: Cambridge University Press. Contribution of Working Group I to the Sixth Assessment Report of the Intergovernmental Panel on Climate Change. URL <https://www.ipcc.ch/report/ar6/wg1/>
- IPCC (2022) Summary for policymakers. In: Shukla, P.R., Skea, J., Slade, R., Al Khourdajie, A., van Diemen, R., McCollum, D. et al. (Eds.) *Climate Change 2022: Mitigation of Climate Change. Contribution of Working Group III to the Sixth Assessment Report of the Intergovernmental Panel on Climate Change*. Cambridge, UK and New York, NY, USA: Cambridge University Press.
- Jacob, D., Teichmann, C., Sobolowski, S., Katragkou, E., Anders, I., Belda, M. et al. (2020) Regional climate downscaling over Europe: perspectives from the EURO-CORDEX community. *Regional Environmental Change*, 20(2), 51. doi:10.1007/s10113-020-01606-9. URL <https://doi.org/10.1007/s10113-020-01606-9>
- Jebeile, J. & Roussos, J. (2023) Usability of climate information: Toward a new scientific framework. *Wiley Interdisciplinary Reviews: Climate Change*, 14(5), e833.
- Kotlarski, S., Gobiet, A., Morin, S., Olefs, M., Rajczak, J. & Samacoits, R. (2023) 21st century alpine climate change. *Climate Dynamics*, 60(1), 65–86.
- Kraemer, M.U., Reiner Jr, R.C., Brady, O.J., Messina, J.P., Gilbert, M., Pigott, D.M. et al. (2019) Past and future spread of the arbovirus vectors aedes aegypti and aedes albopictus. *Nature microbiology*, 4(5), 854–863.
- Kramer, I.M., Pfeiffer, M., Steffens, O., Schneider, F., Gerger, V., Phuyal, P. et al. (2021) The ecophysiological plasticity of aedes aegypti and aedes albopictus concerning overwintering in cooler ecoregions is driven by local climate and acclimation capacity. *Science of the Total Environment*, 778, 146128.
- Kramer, I.M., Pfenninger, M., Feldmeyer, B., Dhimal, M., Gautam, I., Shreshta, P. et al. (2023) Genomic profiling of climate adaptation in aedes aegypti along an altitudinal gradient in Nepal indicates nonradial expansion of the disease vector. *Molecular ecology*, 32(2), 350–368.
- Kuhn, M., Weston, S. & Keefer, C. (2024) Package 'cubist'. *Rule-and Instance-Based Regression Modeling. R Package Version 0.4*, 1.
- Lacour, G. (2016) Eco-physiological mechanisms and adaptive value of egg diapause in the invasive mosquito aedes albopictus (Diptera: Culicidae). *Belgium: Royal Belgian Institute of Natural Sciences*.
- Lacour, G., Vernichon, F., Cadilhac, N., Boyer, S., Lagneau, C. & Hance, T. (2014) When mothers anticipate: effects of the pre-diapause stage on embryo development time and of maternal photoperiod on eggs of a temperate and a tropical strains of aedes albopictus (Diptera: Culicidae). *Journal of Insect Physiology*, 71, 87–96.
- Lang, M., Binder, M., Richter, J., Schratz, P., Pfisterer, F., Coors, S. et al. (2019) mlr3: A modern object-oriented machine learning framework in R. *Journal of Open Source Software*, 4(44), 1903.
- Laverdeur, J., Desmecht, D., Hayette, M.P. & Darcis, G. (2024) Dengue and chikungunya: future threats for northern Europe? *Frontiers in epidemiology*, 4, 1342723.
- Lazoglou, G., Papadopoulos-Zachos, A., Georgiades, P., Zittis, G., Velikou, K., Manios, E.M. et al. (2024) Identification of climate change hotspots in the Mediterranean. *Scientific reports*, 14(1), 29817.
- Li, M.F., Tang, X.P., Wu, W. & Liu, H.B. (2013) General models for estimating daily global solar radiation for different solar radiation zones in mainland China. *Energy conversion and management*, 70, 139–148.
- Li, Y., Kamara, F., Zhou, G., Puthiyakunnon, S., Li, C., Liu, Y. et al. (2014) Urbanization increases aedes albopictus larval habitats and accelerates mosquito development and survivorship. *PLoS neglected tropical diseases*, 8(11), e3301.
- Manica, M., Filipponi, F., D'Alessandro, A., Screti, A., Neteler, M., Rosa, R. et al. (2016) Spatial and temporal hot spots of aedes albopictus abundance inside and outside a South European metropolitan area. *PLoS neglected tropical diseases*, 10(6), e0004758.
- Marini, G., Manica, M., Arnoldi, D., Inama, E., Rosà, R. & Rizzoli, A. (2020) Influence of temperature on the life-cycle dynamics of aedes albopictus population established at temperate latitudes: A laboratory experiment. *Insects*, 11(11), 808.
- Matiu, M., Napoli, A., Kotlarski, S., Zardi, D., Bellin, A. & Majone, B. (2024) Elevation-dependent biases of raw and bias-adjusted EURO-CORDEX regional climate models in the European Alps. *Climate Dynamics*. doi:10.1007/s00382-024-07376-y. URL <https://doi.org/10.1007/s00382-024-07376-y>
- McCain, C.M. & Garfinkel, C.F. (2021) Climate change and elevational range shifts in insects. *Current Opinion in Insect Science*, 47, 111–118.

- McGough, S.F., Brownstein, J.S., Hawkins, J.B. & Santillana, M. (2017) Forecasting zika incidence in the 2016 latin america outbreak combining traditional disease surveillance with search, social media, and news report data. *PLoS neglected tropical diseases*, 11(1), e0005295.
- Medlock, J.M., Hansford, K., Versteirt, V., Cull, B., Kampen, H., Fontenille, D. et al. (2015) An entomological review of invasive mosquitoes in europe. *Bulletin of entomological research*, 105(6), 637–663.
- Metelmann, S., Caminade, C., Jones, A.E., Medlock, J.M., Baylis, M. & Morse, A.P. (2019) The uk's suitability for aedes albopictus in current and future climates. *Journal of the Royal Society Interface*, 16(152), 20180761.
- Molnar, C. (2019) *Interpretable machine learning*. : Lulu.
- Napoli, A., Manti, M., Laiti, L., Barbiero, R., Tombolato, D., Monsorno, S.S. et al. (2026) Building the scientific basis for the adaptation strategy of an alpine region: The 'state of the climate in trentino'report. *Climate Services*, 41, 100629.
- Neteler, M., Metz, M., Rocchini, D., Rizzoli, A., Flacio, E., Engeler, L. et al. (2013) Is switzerland suitable for the invasion of aedes albopictus? *PLoS One*, 8(12), e82090.
- Neteler, M., Roiz, D., Rocchini, D., Castellani, C. & Rizzoli, A. (2011) Terra and aqua satellites track tiger mosquito invasion: modelling the potential distribution of aedes albopictus in north-eastern italy. *International Journal of Health Geographics*, 10(1), 49.
- Paaĳmans, K.P., Heinig, R.L., Seliga, R.A., Blanford, J.I., Blanford, S., Murdock, C.C. et al. (2013) Temperature variation makes ectotherms more sensitive to climate change. *Global change biology*, 19(8), 2373–2380.
- Pacifici, M., Foden, W.B., Visconti, P., Watson, J.E., Butchart, S.H., Kovacs, K.M. et al. (2015) Assessing species vulnerability to climate change. *Nature Climate Change*, 5(3), 215–224.
- Parmesan, C. (2006) Ecological and evolutionary responses to recent climate change. *Annual. Rev. Ecol. Syst.*, 37(1), 637–669.
- Pepin, N., Apple, M., Knowles, J., Terzago, S., Arnone, E., Hanchen, L. et al. (2025) Elevation-dependent climate change in mountain environments. *Nature Reviews Earth & Environment*, 1–17.
- Pepin, N.C., Arnone, E., Gobiet, A., Haslinger, K., Kotlarski, S., No-tarnicola, C. et al. (2022) Climate changes and their elevational patterns in the mountains of the world. *Reviews of geophysics*, 60(1), e2020RG000730.
- Phuyal, P., Kramer, I.M., Klingelhofer, D., Kuch, U., Madeburg, A., Groneberg, D.A. et al. (2020) Spatiotemporal distribution of dengue and chikungunya in the hindu kush himalayan region: a systematic review. *International journal of environmental research and public health*, 17(18), 6656.
- Pichler, M. & Hartig, F. (2023) Machine learning and deep learning—a review for ecologists. *Methods in Ecology and Evolution*, 14(4), 994–1016.
- Proestos, Y., Christophides, G., Erguler, K., Tanarhte, M., Waldock, J. & Lelieveld, J. (2015) Present and future projections of habitat suitability of the asian tiger mosquito, a vector of viral pathogens, from global climate simulation. *Philosophical Transactions of the Royal Society B: Biological Sciences*, 370(1665), 20130554.
- R Core Team (2025) *R: A Language and Environment for Statistical Computing*. R Foundation for Statistical Computing, Vienna, Austria.
URL <https://www.R-project.org/>
- Radici, A., Hammami, P., Cannet, A., L'Ambert, G., Lacour, G., Fournet, F. et al. (2025) Aedes albopictus is rapidly invading its climatic niche in france: Wider implications for biting nuisance and arbovirus control in western europe. *Global Change Biology*, 31(8), e70414.
- Reinhold, J.M., Lazzari, C.R. & Lahondere, C. (2018) Effects of the environmental temperature on aedes aegypti and aedes albopictus mosquitoes: A review. *Insects*, 9(4), doi:10.3390/insects9040158.
URL <https://www.mdpi.com/2075-4450/9/4/158>
- Roiz, D., Neteler, M., Castellani, C., Arnoldi, D. & Rizzoli, A. (2011) Climatic factors driving invasion of the tiger mosquito (aedes albopictus) into new areas of trentino, northern italy. *PLoS one*, 6(4), e14800.
- Roiz, D., Pontifes, P.A., Jourdain, F., Diagne, C., Leroy, B., Vaissiere, A.C. et al. (2024) The rising global economic costs of invasive aedes mosquitoes and aedes-borne diseases. *Science of the Total Environment*, 933, 173054.
- Romiti, F., Casini, R., Magliano, A., Ermenegildi, A. & De Liberato, C. (2022) Aedes albopictus abundance and phenology along an altitudinal gradient in lazio region (central italy). *Parasites & Vectors*, 15(1), 92.
- Romiti, F., Ermenegildi, A., Magliano, A., Rombola, P., Varrenti, D., Giammattei, R. et al. (2021) Aedes albopictus (diptera: Culicidae) monitoring in the lazio region (central italy). *Journal of Medical Entomology*, 58(2), 847–856.
- Schaffner, F., Versteirt, V. & Medlock, J. (2014) Guidelines for the surveillance of native mosquitoes in europe. *ECDC: Stockholm*.
- Semenza, J.C. & Paz, S. (2021) Climate change and infectious disease in europe: Impact, projection and adaptation. *The Lancet Regional Health–Europe*, 9.
- Sherpa, S., Blum, M.G. & Despres, L. (2019) Cold adaptation in the asian tiger mosquito's native range precedes its invasion success in temperate regions. *Evolution*, 73(9), 1793–1808.
- Sherpa, S., Tutagata, J., Gaude, T., Laporte, F., Kasai, S., Ishak, I.H. et al. (2022) Genomic shifts, phenotypic clines, and fitness costs associated with cold tolerance in the asian tiger mosquito. *Molecular Biology and Evolution*, 39(5), msac104.
- Shin, S., Kang, D., Lee, J., Do, M.S., Kang, H.G., Suh, J.H. et al. (2023) Climate warming induces the activity period prolongation and distribution range expansion of the asian mantis hierodula patellifera in south korea. *Journal of Asia-Pacific Entomology*, 26(4), 102162.
- Steiger, R., Knowles, N., Poll, K. & Rutty, M. (2024) Impacts of climate change on mountain tourism: A review. *Journal of Sustainable Tourism*, 32(9), 1984–2017.
- Tatem, A.J., Rogers, D.J. & Hay, S.I. (2006) Global transport networks and infectious disease spread. *Advances in parasitology*, 62, 293–343.
- Thomas, S.M., Obermayr, U., Fischer, D., Kreyling, J. & Beierkuhnlein, C. (2012) Low-temperature threshold for egg survival of a post-diapause and non-diapause european aedine strain, aedes albopictus (diptera: Culicidae). *Parasites & vectors*, 5(1), 100.
- Thuiller, W., Gueĳuen, M., Renaud, J., Karger, D.N. & Zimmermann, N.E. (2019) Uncertainty in ensembles of global biodiversity scenarios. *Nature communications*, 10(1), 1446.
- Tippelt, L., Werner, D. & Kampen, H. (2019) Tolerance of three aedes albopictus strains (diptera: Culicidae) from different geographical origins towards winter temperatures under field conditions in northern germany. *PLoS One*, 14(7), e0219553.
- Tippelt, L., Werner, D. & Kampen, H. (2020) Low temperature tolerance of three aedes albopictus strains (diptera: Culicidae) under constant and fluctuating temperature scenarios. *Parasites & Vectors*, 13(1), 587.
- Tisseuil, C., Velo, E., Bino, S., Kadriaj, P., Mersini, K., Shukullari, A. et al. (2018) Forecasting the spatial and seasonal dynamic of aedes albopictus oviposition activity in albania and balkan countries. *PLoS Neglected Tropical Diseases*, 12(2), e0006236.
- Toma, L., Severini, F., Di Luca, M., Bella, A. & Romi, R. (2003) Seasonal patterns of oviposition and egg hatching rate of aedes albopictus in rome. *J Am Mosq Control Assoc*, 19(1), 100.
- Torina, A., La Russa, F., Blanda, V., Peralbo-Moreno, A., Casades-Marti, L., Di Pasquale, L. et al. (2023) Modelling time-series aedes albopictus abundance as a forecasting tool in urban environments. *Ecological Indicators*, 150, 110232.
- Westby, K.M., Adalsteinsson, S.A., Biro, E.G., Beckermann, A.J. & Medley, K.A. (2021) Aedes albopictus populations and larval habitat characteristics across the landscape: Significant differences

exist between urban and rural land use types. *Insects*, 12(3), 196.

Wilke, A.B., Benelli, G. & Beier, J.C. (2021) Anthropogenic changes and associated impacts on vector-borne diseases. *Trends in parasitology*, 37(12), 1027–1030.

Wolpert, D.H. (1992) Stacked generalization. *Neural networks*, 5(2), 241–259.

How to cite this article: Blaha M, Matiu M C, Majone B, Zardi D, Flacio E, Anicic N, Swiss Mosquito Network, Rizzoli A, Stenico A, Cassina F, Rosà R, and Da Re D. Climate-driven shifts in the population dynamics of the invasive Asian tiger mosquito (*Aedes albopictus*) in the Alps *Global Change Biology* 2026;00(00):1–18.

APPENDIX

A SUPPLEMENTARY METHODS AND RESULTS

TABLE A1 Summary of ovitrap monitoring effort and data coverage by region. The table reports temporal coverage, number of original monitoring stations, total number of weekly observations, mean sampling intensity per year, number of grid cells after spatial aggregation, and elevation range of monitoring locations.

Region	Years covered	N sampling loc.	N obs	Mean obs / year	Grid cells	Min elev. (m)	Max elev. (m)
Autonomous Province of Bolzano (IT)	2013–2024	221	81,982	7,453	18	255	1,871
Autonomous Province of Trento (IT)	2010–2022	15	6,421	494	15	6	1,356
Emilia–Romagna (IT)	2010–2024	1,217	481,124	32,075	42	–10	205
Espace Mittelland (CH)	2022–2024	7	423	212	3	528	669
Nordwestschweiz (CH)	2022–2024	131	7,931	2,644	7	275	669
Ostschweiz (CH)	2022–2024	121	11,249	3,750	15	438	2,562
Région lémanique (CH)	2022–2024	72	5,272	1,757	7	366	720
Ticino (CH)	2010–2024	276	23,944	1,596	14	245	1,559
Veneto (IT)	2018–2022	18	2,863	573	18	–3	1,942
Zentralschweiz (CH)	2023–2024	3	159	79.5	1	727	727
Zürich (CH)	2023–2024	10	530	265	2	401	550

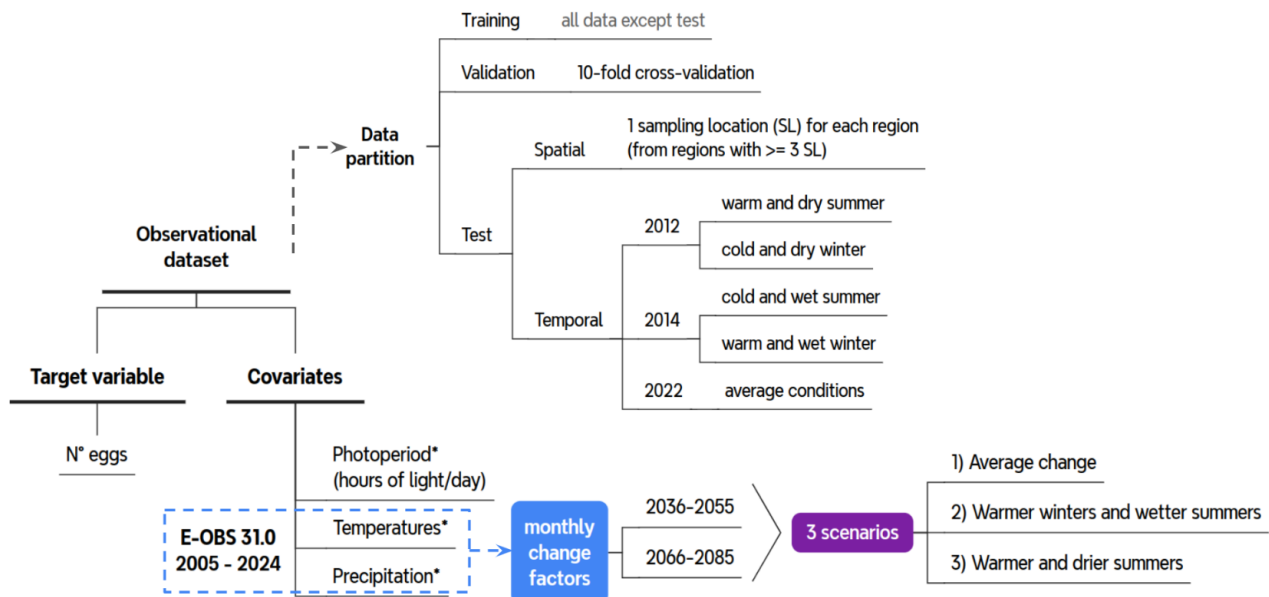


FIGURE A1 Workflow for integrating ovitrap and environmental data. Meteorological variables from the E-OBS v31.0 dataset are aggregated to weekly resolution, and temporal lags are calculated using rolling means to account for the short-term delayed effects of environmental conditions on mosquito populations. Ovitrap data are temporally standardised and spatially aggregated to align with the resolution of the environmental data. The two data streams are then joined to produce the final dataset for modelling, which is subdivided into training set and two testing sets. After training and testing, the model is applied to the covariates adjusted for climate change under the RCP8.5 scenario.

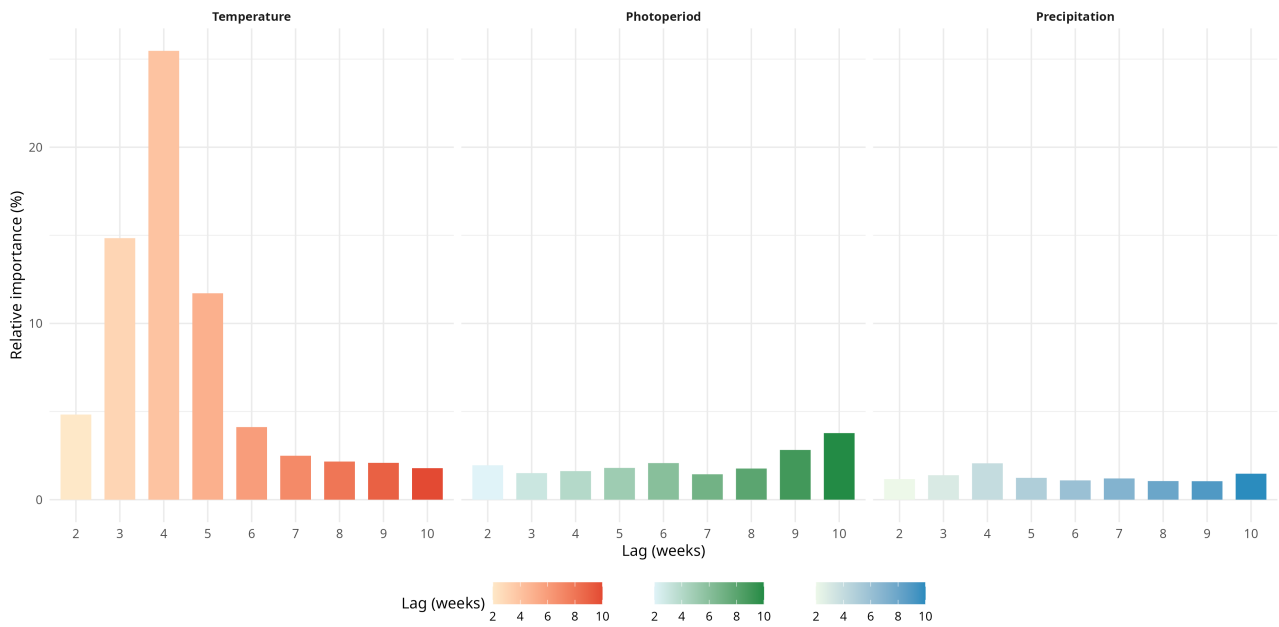


FIGURE A2 Relative importance of environmental predictors in the machine-learning model. Bars show the percentage contribution of lagged temperature, photoperiod, and precipitation variables to the Random Forest model performance.

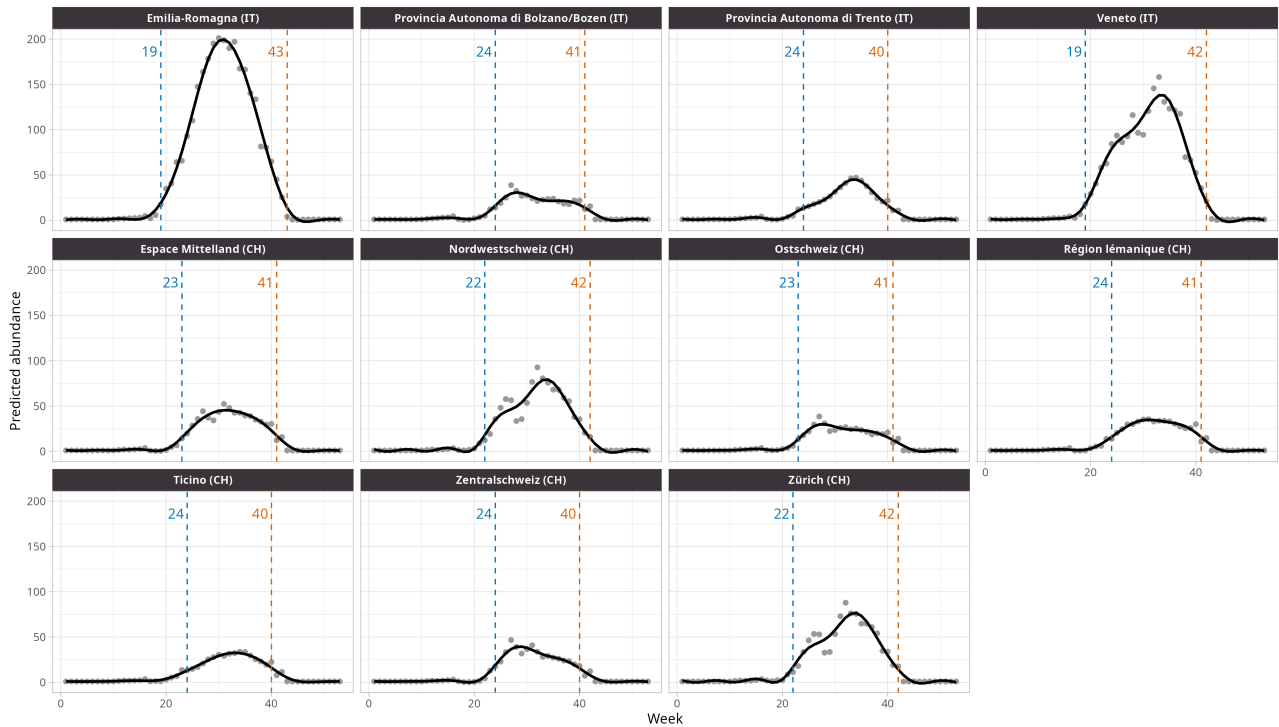


FIGURE A3 Current seasonal dynamics predicted for *Ae. albopictus* egg abundance across regions in northern Italy and Switzerland. Mean predicted weekly abundance for each region in current conditions (points) is shown alongside smoothed seasonal curves (black lines). Vertical dashed lines indicate the start (blue) and end (orange) of the activity period, defined as the first and last weeks when predicted abundance exceeds a threshold of 5% of the maximum observed mean across all regions. Labels above the curves indicate the corresponding week numbers for activity onset and termination.

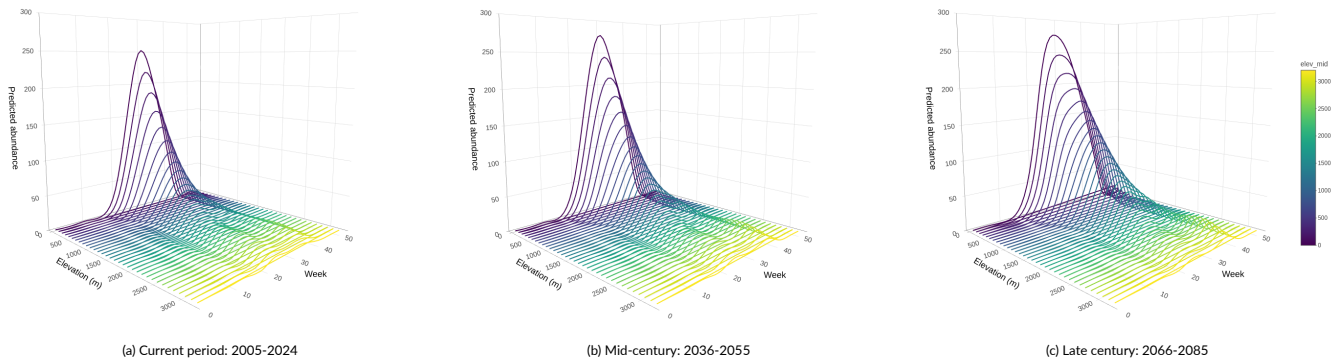
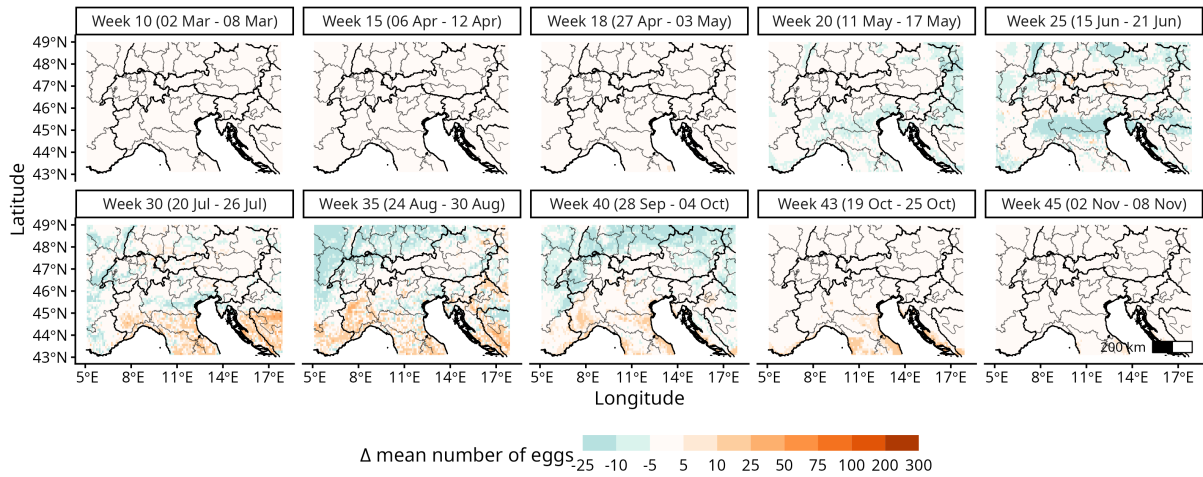
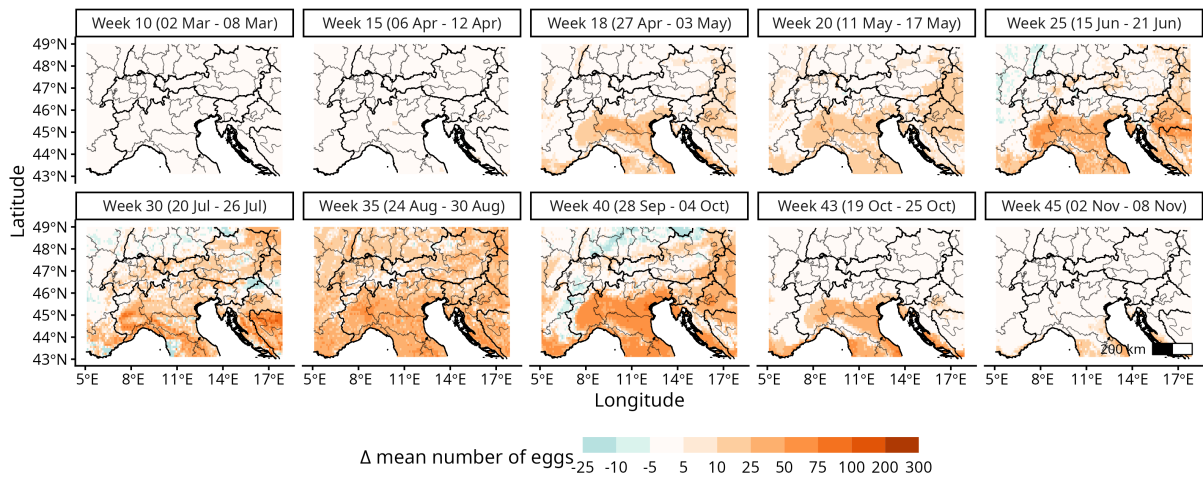


FIGURE A4 Seasonal and elevational dynamics of *Ae. albopictus* egg abundance under current and future climate. Generalized additive models (GAMs) were fitted to weekly predicted abundances across 100 m elevational bands for (a) current conditions, (b) mid-century (2036–2055), and (c) late-century (2066–2085) projections. Surface plots (colored by elevation) illustrate predicted abundance across the seasonal cycle (weeks 1–53) and the elevational gradient, while overlaid lines represent smoothed GAM predictions for each elevational band. These figures help visualise both temporal shifts (timing and width of the active season) and spatial shifts (expansion to higher elevations) under projected climate change. The z-axis represents predicted egg abundance. Notably, future climates show extended activity periods and higher predicted abundance at higher elevations compared with current conditions.

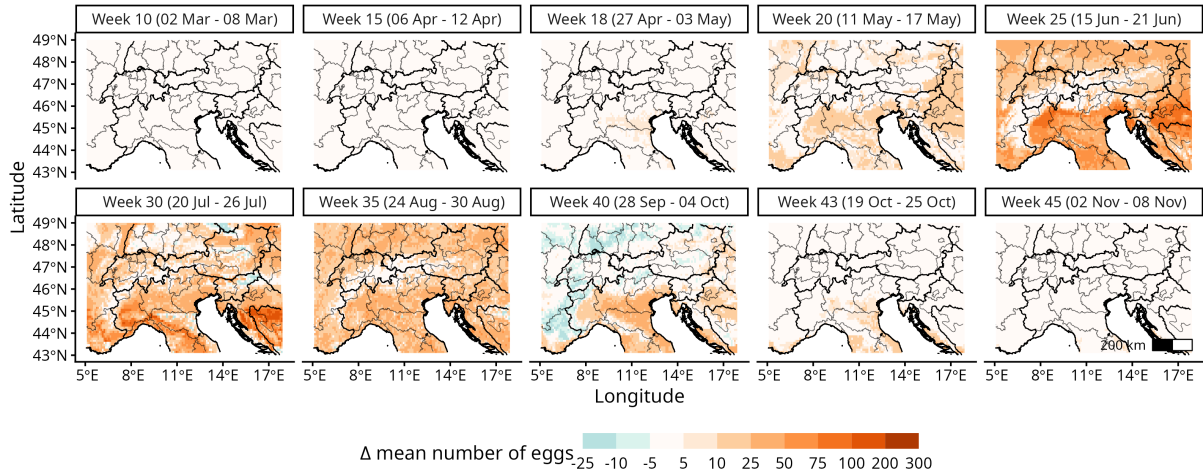


(a) Change in predicted egg abundance in the (2) Warmer winters & wetter summers configuration during the mid-century (2036–2055) relative to the current baseline.

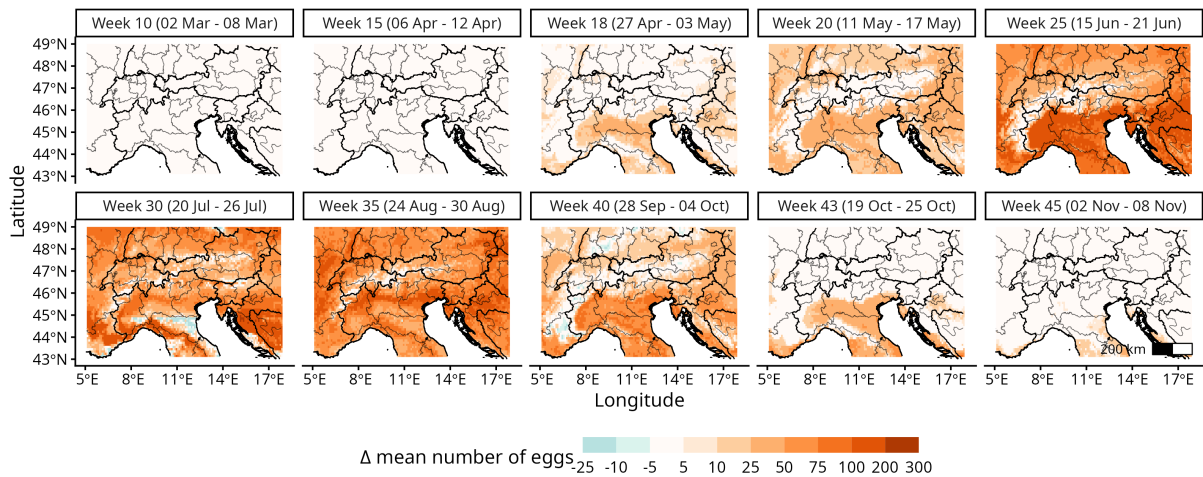


(b) Change in predicted egg abundance in the (2) Warmer winters & wetter summers configuration during the late-century (2055–2086) relative to the current baseline.

FIGURE A5 Spatial projections of changes in *Ae. albopictus* egg abundance under the Warmer winters & wetter summers future. Panel (a) shows the mid-century period (2036–2055) relative to the current baseline, while panel (b) shows the late-century period (2055–2086). Positive values indicate increases in predicted egg abundance, and negative values indicate decreases.



(a) Change in predicted egg abundance in the (3) Warmer & drier summers configuration during the mid-century (2035-2066) relative to the current baseline.



(b) Change in predicted egg abundance in the (3) Warmer & drier summers configuration during the late-century (2055-2086) relative to the current baseline.

FIGURE A6 Spatial projections of changes in *Ae. albopictus* egg abundance under the Warmer & drier summers future. Panel (a) shows the mid-century period (2035-2066) relative to the current baseline, while panel (b) shows the late-century period (2055-2086). Positive values indicate increases in predicted egg abundance, and negative values indicate decreases.

TABLE A2: Mean (\pm SD) of simulated *Ae. albopictus* season length (weeks) by region, period, and climate.

Region	Period	Climate future	Mean season length (weeks \pm SD)
Autonomous Province of Bolzano (IT)	2005–2024	Current period	18.55 \pm 4.38
	2036–2055	(1) Average change	19.73 \pm 4.08
	2036–2055	(2) Warmer winters & wetter summers	18.73 \pm 3.71
	2036–2055	(3) Warmer & drier summers	19.82 \pm 3.43
	2066–2085	(1) Average change	21.41 \pm 3.49
	2066–2085	(2) Warmer winters & wetter summers	19.86 \pm 4.09
	2066–2085	(3) Warmer & drier summers	21.82 \pm 2.11
Autonomous Province of Trento (IT)	2005–2024	Current period	19.32 \pm 3.07
	2036–2055	(1) Average change	21.32 \pm 2.08
	2036–2055	(2) Warmer winters & wetter summers	19.42 \pm 2.97
	2036–2055	(3) Warmer & drier summers	20.84 \pm 2.12
	2066–2085	(1) Average change	22.89 \pm 3.00
	2066–2085	(2) Warmer winters & wetter summers	21.32 \pm 2.45
	2066–2085	(3) Warmer & drier summers	22.68 \pm 2.19
Emilia-Romagna (IT)	2005–2024	Current period	23.36 \pm 2.98
	2036–2055	(1) Average change	25.21 \pm 2.94
	2036–2055	(2) Warmer winters & wetter summers	22.93 \pm 3.34
	2036–2055	(3) Warmer & drier summers	24.14 \pm 2.66
	2066–2085	(1) Average change	28.07 \pm 3.50
	2066–2085	(2) Warmer winters & wetter summers	25.71 \pm 3.36
	2066–2085	(3) Warmer & drier summers	25.93 \pm 2.79
Espace Mittelland (CH)	2005–2024	Current period	18.00 \pm 4.55
	2036–2055	(1) Average change	20.35 \pm 1.04
	2036–2055	(2) Warmer winters & wetter summers	18.15 \pm 2.91
	2036–2055	(3) Warmer & drier summers	18.80 \pm 3.87
	2066–2085	(1) Average change	21.10 \pm 1.62
	2066–2085	(2) Warmer winters & wetter summers	19.95 \pm 1.00
	2066–2085	(3) Warmer & drier summers	20.65 \pm 3.08
Nordwestschweiz (CH)	2005–2024	Current period	21.75 \pm 0.96
	2036–2055	(1) Average change	23.25 \pm 1.26
	2036–2055	(2) Warmer winters & wetter summers	21.25 \pm 0.50
	2036–2055	(3) Warmer & drier summers	22.25 \pm 0.50
	2066–2085	(1) Average change	25.00 \pm 0.82
	2066–2085	(2) Warmer winters & wetter summers	22.75 \pm 1.50
	2066–2085	(3) Warmer & drier summers	25.00 \pm 1.15
Ostschweiz (CH)	2005–2024	Current period	17.54 \pm 4.79
	2036–2055	(1) Average change	18.75 \pm 4.32
	2036–2055	(2) Warmer winters & wetter summers	16.88 \pm 4.78
	2036–2055	(3) Warmer & drier summers	18.54 \pm 4.20
	2066–2085	(1) Average change	21.38 \pm 1.86
	2066–2085	(2) Warmer winters & wetter summers	19.79 \pm 3.19
	2066–2085	(3) Warmer & drier summers	21.33 \pm 2.08
	2005–2024	Current period	18.79 \pm 3.21

Continued on next page

Region	Period	Climate future	Mean season length (weeks \pm SD)
	2036–2055	(1) Average change	20.14 \pm 2.09
	2036–2055	(2) Warmer winters & wetter summers	18.68 \pm 2.00
	2036–2055	(3) Warmer & drier summers	19.04 \pm 3.35
	2066–2085	(1) Average change	20.82 \pm 2.60
	2066–2085	(2) Warmer winters & wetter summers	19.64 \pm 2.75
	2066–2085	(3) Warmer & drier summers	20.50 \pm 3.43
Ticino (CH)	2005–2024	Current period	17.94 \pm 4.78
	2036–2055	(1) Average change	19.17 \pm 5.27
	2036–2055	(2) Warmer winters & wetter summers	18.50 \pm 3.79
	2036–2055	(3) Warmer & drier summers	18.83 \pm 4.84
	2066–2085	(1) Average change	22.39 \pm 4.13
	2066–2085	(2) Warmer winters & wetter summers	21.11 \pm 3.16
Veneto (IT)	2005–2024	Current period	19.45 \pm 5.39
	2036–2055	(1) Average change	22.82 \pm 3.23
	2036–2055	(2) Warmer winters & wetter summers	20.18 \pm 4.34
	2036–2055	(3) Warmer & drier summers	21.64 \pm 3.65
	2066–2085	(1) Average change	24.59 \pm 4.62
	2066–2085	(2) Warmer winters & wetter summers	22.64 \pm 4.26
Zentralschweiz (CH)	2005–2024	Current period	16.35 \pm 4.16
	2036–2055	(1) Average change	18.45 \pm 3.75
	2036–2055	(2) Warmer winters & wetter summers	15.70 \pm 3.54
	2036–2055	(3) Warmer & drier summers	17.05 \pm 3.97
	2066–2085	(1) Average change	20.15 \pm 3.42
	2066–2085	(2) Warmer winters & wetter summers	18.40 \pm 3.44
Zürich (CH)	2005–2024	Current period	21.75 \pm 0.96
	2036–2055	(1) Average change	22.50 \pm 0.58
	2036–2055	(2) Warmer winters & wetter summers	20.75 \pm 0.50
	2036–2055	(3) Warmer & drier summers	22.50 \pm 0.58
	2066–2085	(1) Average change	24.75 \pm 0.50
	2066–2085	(2) Warmer winters & wetter summers	21.75 \pm 0.50
2066–2085	(3) Warmer & drier summers	24.50 \pm 1.29	

B CLIMATE DATA PROCESSING

B.1 Extreme year selection for temporal validation

We selected the extreme years based on the ML model covariates. For this we averaged temperature and summer precipitation seasonally for each location ID and then averaged spatially for each year (2010–2024). We then applied the method from Cannon (2015), which selects the global centroid of the result space and then sequentially the $(k-1)$ elements of the ensemble that are the farthest from the global centroid in the result space. The result space here is composed of the seasonal values of temperature and precipitation for all the years, that is a matrix with 15 rows (one for each year) and 8 columns (2 variables times 4 seasons). For $k=5$, the resulting selection is shown in Figure B7. The year 2022 is the resulting global centroid, representing the approximate average year. 2012 has the warmest and driest summer coupled with a cold and dry winter, while 2014 has the coldest and second-wettest summer coupled with the warmest and wettest winter.

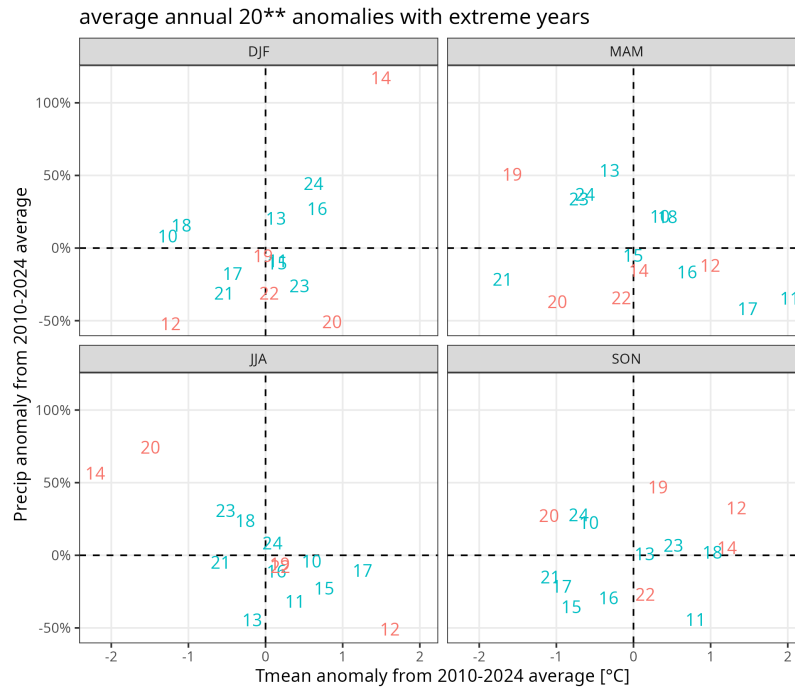


FIGURE B7 Seasonal values of temperature and precipitation for each year as anomaly over the full 2010-2024 period. The highlighted years are identified as most extreme years.

B.2 RCM sub-ensemble

To select a sub-ensemble from the RCMs, we applied the same procedure as above. Here the result space consisted of the climate change deltas for the period 2066-2085 with respect to 2006-2025, averaged over the whole domain, for summer (JJA) and winter (DJF) only. This results in a input matrix with the number of GCM-RCMs as rows and four columns: 1) winter temperature, 2) summer temperature, 3) winter precipitation, and 4) summer precipitation. Choosing three models allowed us to capture 80% of the total spread in the expected changes of these four variables. Figure B8 shows the result space and selected models. The model 1, which represents the ensemble average (average warming, slightly drier summers, slightly wetter winters), is DMI-HIRHAM5 driven by MOHC-HadGEM2-ES. Model 2, which represents warm winters with cold-wet summers, is IPSL-WRF381P driven by IPSL-IPSL-CM5A-MR. Model 3, which represents hot-dry summers and less warm winters, is MOHC-HadREM3-GA7-05 driven by ICHEC-EC-EARTH. Figure B9 shows the changes of the selected models only for both periods and all four seasons; note that the model selection was based only on the last period DJF and JJA.

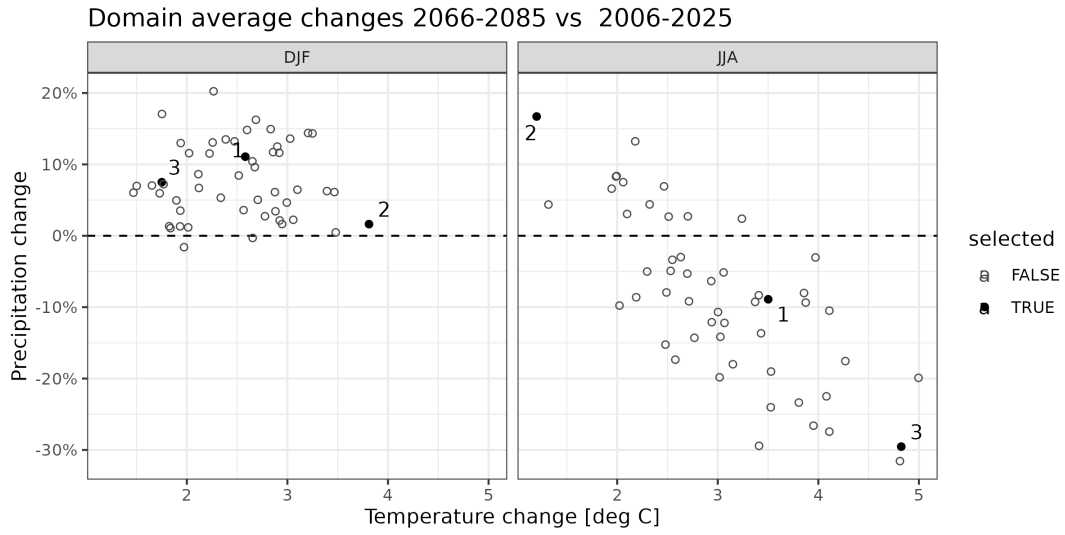


FIGURE B8 Sub-ensemble selection based on climate change deltas. Each points is a different regional climate model. The labels refer to the same model in the two selected seasons (DJF and JJA).

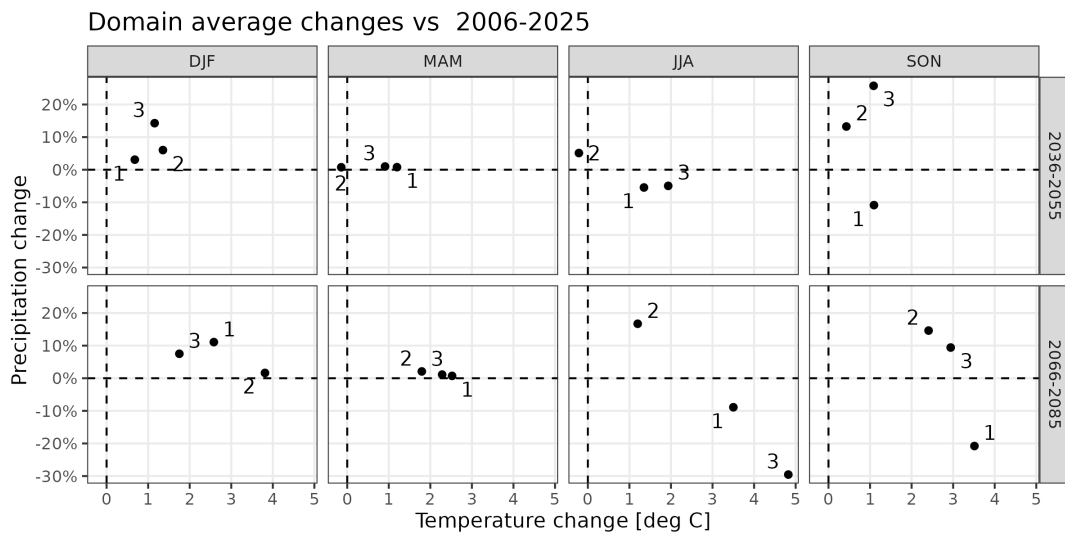


FIGURE B9 Seasonal changes for the selected climate models in the sub-ensemble.